A TECHNIQUE FOR MEASURING UNSTEADY PRESSURES

by

Ronald Bruce Johnson

UNITED STATES
NAVAL POSTGRADUATE SCHOOL

THESIS

A TECHNIQUE FOR MEASURING UNSTEADY PRESSURES

by

Ronald Bruce Johnson

September 1968

A TECHNIQUE FOR MEASURING UNSTEADY PRESSURES

by

Ronald Bruce Johnson
Lieutenant, United States Navy
B.S., The University of Washington, 1960

Submitted in partial fulfillment of the
requirements for the degree of

AERONAUTICAL ENGINEER

from the

NAVAL POSTGRADUATE SCHOOL
September 1968

ABSTRACT

A system for measuring unsteady pressures in flow fields employing a remote transducer and thin plastic pressure transmitting lines has been designed and built.

The static and dynamic characteristics of the system were determined experimentally, and the results were found to agree well with a theoretical model.

The measuring system was subsequently integrated into a two-dimensional wind tunnel model consisting of a symmetrical airfoil with a plain oscillating flap. The flap was harmonically oscillated, and the measuring system was used to determine both the steady and unsteady pressures at a point near the flap hinge line. The static and dynamic results were then compared to those obtained using thin airfoil theory and found to agree well when corrected for thickness effects.

TABLE OF CONTENTS

LIST OF TABLES

LIST OF FIGURES

TABLE OF SYMBOLS

Latin Symbols

a_o	Mean velocity of sound
c	Airfoil chord
C_p	Specific heat at constant pressure
ΔC_p	Pressure coefficient across airfoil (non-dimensional) = $\frac{\Delta p}{q}$
C_v	Specific heat at constant volume
D	Tube inside diameter
g	Gravity constant
i	Imaginary unit = $\sqrt{-1}$
J_n	Bessel function of first kind of order n
k	Polytropic constant for volumes
k	Non-dimensional frequency = $\frac{\omega c}{2U}$
L	Length of flexible tube
$\bar{P}$	Static pressure, including steady and unsteady terms
P_o	Mean pressure
P	Amplitude of pressure disturbance
P_1	Driving pressure
P_2	Measured pressure (transducer sensed)
P_L	Pressure on airfoil lower surface
P_u	Pressure on airfoil upper surface
Pr	Prandtl number = $\frac{\mu g C_p}{\lambda}$
q	Dynamic pressure = $\frac{1}{2} \rho U^2$
r	Radial coordinate
R	Tube radius
$\bar{R}$	Gas constant
t	Time

$\bar{T}$	Combined temperature inside tube, steady plus unsteady component
To	Mean temperature inside tube
T	Amplitude of temperature disturbance inside tube
$\bar{u}$	Complex velocity component in axial direction inside tube
u	Amplitude of velocity component in axial direction inside tube
U	Velocity of fluid meeting the airfoil
$\bar{v}$	Complex velocity component in radial direction inside tube
v	Amplitude of velocity component in radial direction inside tube
V_v	Volume of pressure transducer
V_t	Tube volume

Greek Symbols

α	Wave number (Equation 6)
β	Location of chordal station in transformed coordinates
γ	Ratio of specific heats = $\frac{C_p}{C_v}$
δ	Control surface deflection, positive deflection trailing edge down
θ	Phase angle
λ	Coefficient of thermal conductivity
μ	Absolute fluid viscosity
ψ	Location of hinge line station in transformed coordinates
ω	Frequency
$\bar{\rho}$	Fluid density
ρ_o	Mean fluid density
ρ	Amplitude of fluid density disturbance
τ	Time constant

CHAPTER I

INTRODUCTION

There is a clear need for a practical and inexpensive technique to measure unsteady pressures on experimental models. The character of the pressures being measured may be either well defined and harmonic, as might be found on an oscillating airfoil, or random natured as found in the separated flow region of flow about a bluff body. Although progress has been made in the fabrication of small light weight transducers which may be installed directly in a model, the problem remains of accounting for the model dynamic effects on the transducer response. Two other factors limit the use of this type of system: space limitations, such as those encountered when working with a thin airfoil, and the important factor of cost.

It is a commonly accepted technique to use long thin pressure leads to connect a static orifice to a centrally located pressure sensing instrument such as a manometer board, a micromanometer, or an electrical pressure transducer for the purpose of measuring average pressure. Although it is apparently not well known in this country, a suitably sized pressure lead used in conjunction with a properly selected transducer cavity volume will also provide adequate dynamic response traits so as to be useful for measuring unsteady pressure.

Bergh [1] at the National Aeronautical and Astronautical Research Institute (N.L.R.) in Amsterdam, Holland, has demonstrated a technique that employs long thin pressure leads for the measurement of unsteady pressures. He has presented measurements of the in-phase and out-of-phase pressure distributions on harmonically oscillating Tee-tail configurations in a sub-sonic wind tunnel. The

technique employs multiple pressure leads, having identical dynamic traits, consecutively sampled in a scanning valve arrangement by a single pressure transducer system. Similar methods have been employed by Laschka [2] on a moving rigid model at the Entwicklungsrings Sud in Munich, Germany, with good agreement between theory and experiment. Although employed in European laboratories, this technique has apparently not been used to any extent in this country.

It was the purpose of the investigation described herein to confirm the results of Bergh [1,3] by direct frequency response measurements upon a home built pressure measuring system and then apply the technique of measurement to a typical unsteady flow environment. For the latter purpose, a two-dimensional airfoil model with an oscillating plain flap was designed and instrumented with pressure orifices just ahead of the hinge line. The results obtained experimentally are then compared to those obtained using thin airfoil theory.

Because of a concern for using the technique in environments other than harmonic flow, the indicial response traits of the system have also been determined.

CHAPTER II

EXPERIMENTAL EQUIPMENT AND PROCEDURES

I. EQUIPMENT

General

The work described here was conducted in the Dynamics Laboratory and the 3.5 foot by 5.0 foot wind tunnel of the Naval Postgraduate School's Aeronautical Engineering Laboratories.

The dynamics laboratory provided the work area for construction and calibration of the locally prepared pressure pickups. The wind tunnel provided a place to demonstrate the pressure measuring method on a practical model, in this case, a two-dimensional flapped airfoil.

Pressure Transducers

The pressure pickups employed in the study described here were fabricated from a local design shown in Figure 1. The transducer assembly consisted of a Bentley Nevada Corporation Model D-252 Distance Detector system, a brass sensing head holder and a 0.003 inch thick annealed brass diaphragm. The Distance Detector system was composed of a D-252 Distance Detector, a 15 volt direct current regulated power supply and a H-1-022-4 sensing head.

The distance detector system is a reluctance gage which senses changes in reluctance produced by changes in air gap between the sensing head coil face and the surface of a conducting material. Brass was chosen as the diaphragm material in this case due to its availability and ease of fabrication. Other materials which could equally well have been used as a reference include gold, silver, platinum, copper and aluminum.

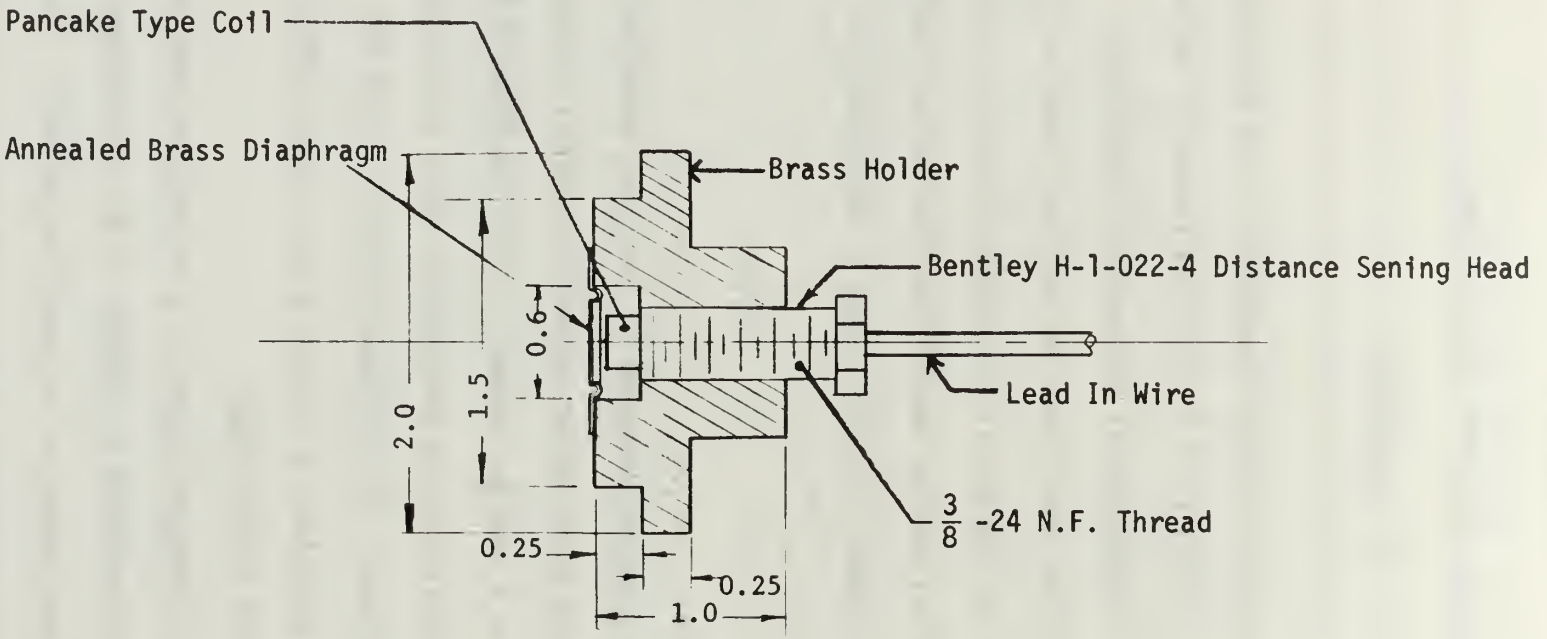

NOTE

1. All Dimensions in Inches

FIGURE 1 SECTIONAL DRAWING OF PRESSURE TRANSDUCER

The annealed brass diaphragm was press formed, cut to size and sweat soldered to the face of the brass sensing head holder. Brass was selected for the sensing head holder in order to reduce differential expansion effects caused by thermal changes. After the diaphragm was attached to the holder, the sensing head was inserted in the holder as may be seen in Figures 1 and 2 which show the pressure transducer.

During the initial stages of transducer construction a diaphragm thickness of 0.003 inches was chosen. The choice of diaphragm thickness was based upon the need for a high sensitivity in the pressure range, referred to ambient, of plus or minus 1.0 pound per square inch (p.s.i.). The transducer constructed for use here is similar to one used by Schmidt [4] in an investigation of fluctuating air loads.

Calibration Chamber and Transducer Holders

The calibration chamber was designed to determine the static and dynamic characteristics of the pressure transducer systems. It was constructed of an aluminum block 4 inches long with a 1.5 inch diameter cylindrical chamber in the center and is shown in Figure 3. The chamber had both ends faced and counter bored to accept either a transducer or an adapter plate used to connect the chamber to a pressure line. Two additional openings were provided in the calibration chamber: one to accept an acoustical driver unit, in this case a University Sound ID-75 Driver Unit, and the other a pressure port to enable the mean static pressure in the chamber to be varied. The acoustic driver unit was placed at the midpoint of the acoustic cavity length so that unsteady pressure pulses could be introduced symmetrically into the cavity.

FIGURE 2 PRESSURE TRANSDUCER

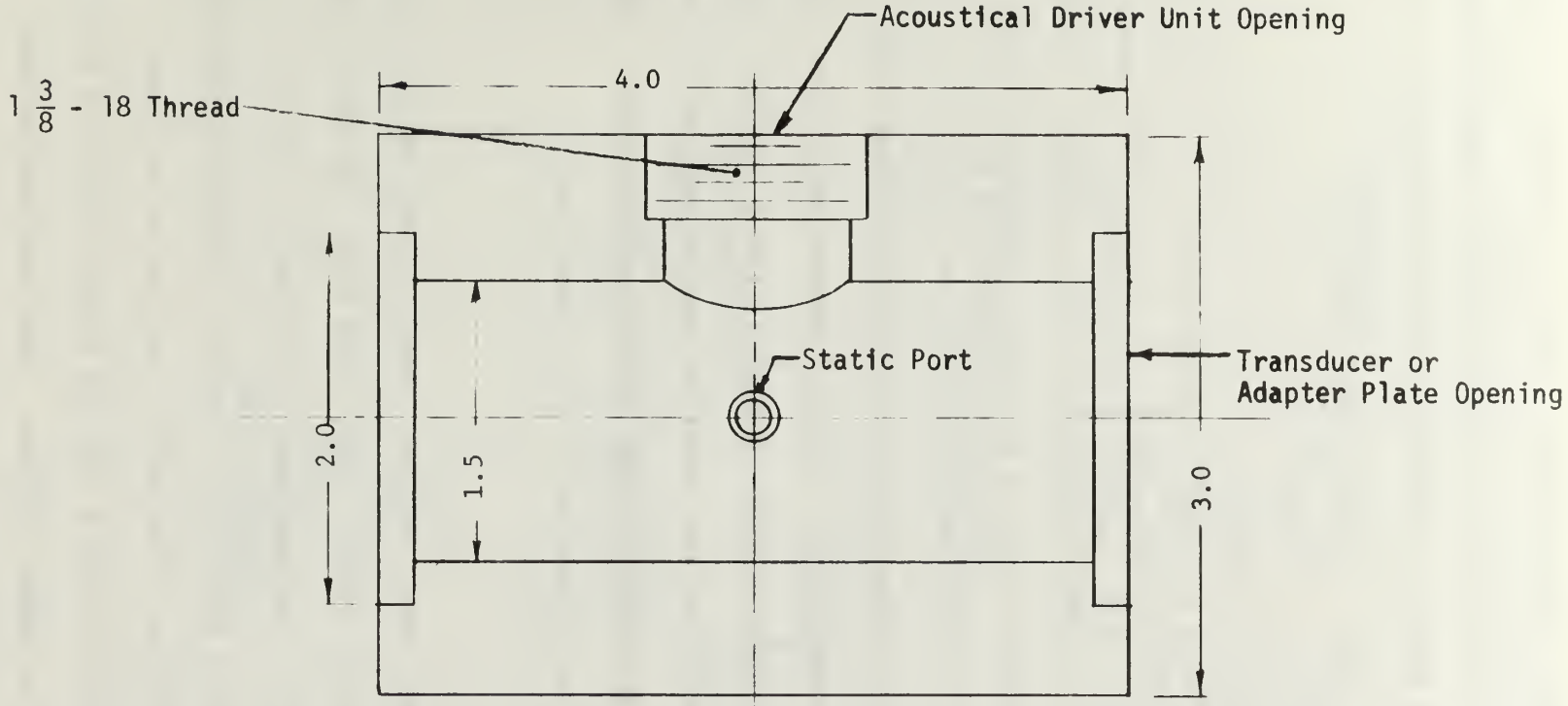

NOTES
1. All Dimensions in Inches
2. Machined from 4.0x3.0x3.0 Aluminum Block

FIGURE 3 SECTIONAL DRAWING OF THE TRANSDUCER CALIBRATION CHAMBER

During static calibration both transducers were installed directly in the chamber, while for the dynamic calibration the adapter plate was placed over one end of the chamber and the remote transducer placed in a suitable holder. The holder was then connected to the calibration chamber using a flexible Tygon tube

Instrumentation

The output from a pressure transducer was fed into an Astro-Data Model D-885 amplifier. The output from the Astro-Data amplifier was read on a United Systems Corporation, Digitec, digital voltmeter for the static calibration and on a Ballentine Laboratories Model 320A True root mean square (R.M.S) meter during dynamic calibration. During dynamic calibration the signal from a Hewlett Packard Model 200CD wide range oscillator was amplified by a General Radio Company Type 1233-A power amplifier and used to actuate the acoustical driver unit, and an AD-YU Type 405 precision phase meter was used to measure the phase difference between the output voltages of the two transducers. The instrumentation is shown schematically in Figures 4 and 5.

Wind Tunnel Model

The wind tunnel model used was a modified NACA 64_1-012 airfoil with a 20 per cent chord, radius nosed, plain flap. The model had a span of 22 inches with a constant chord of 12 inches The tips of the model were terminated in end plates in order to simulate two-dimensional flow traits. Modification of the airfoil section was achieved by straight line fairing the surface from the 60 per cent chord position to the trailing edge to remove the cusp. Two flush mounted static pressure taps were installed on the upper and lower surfaces of the airfoil 0.6 inches ahead of the flap hinge line (0.75 per cent chord

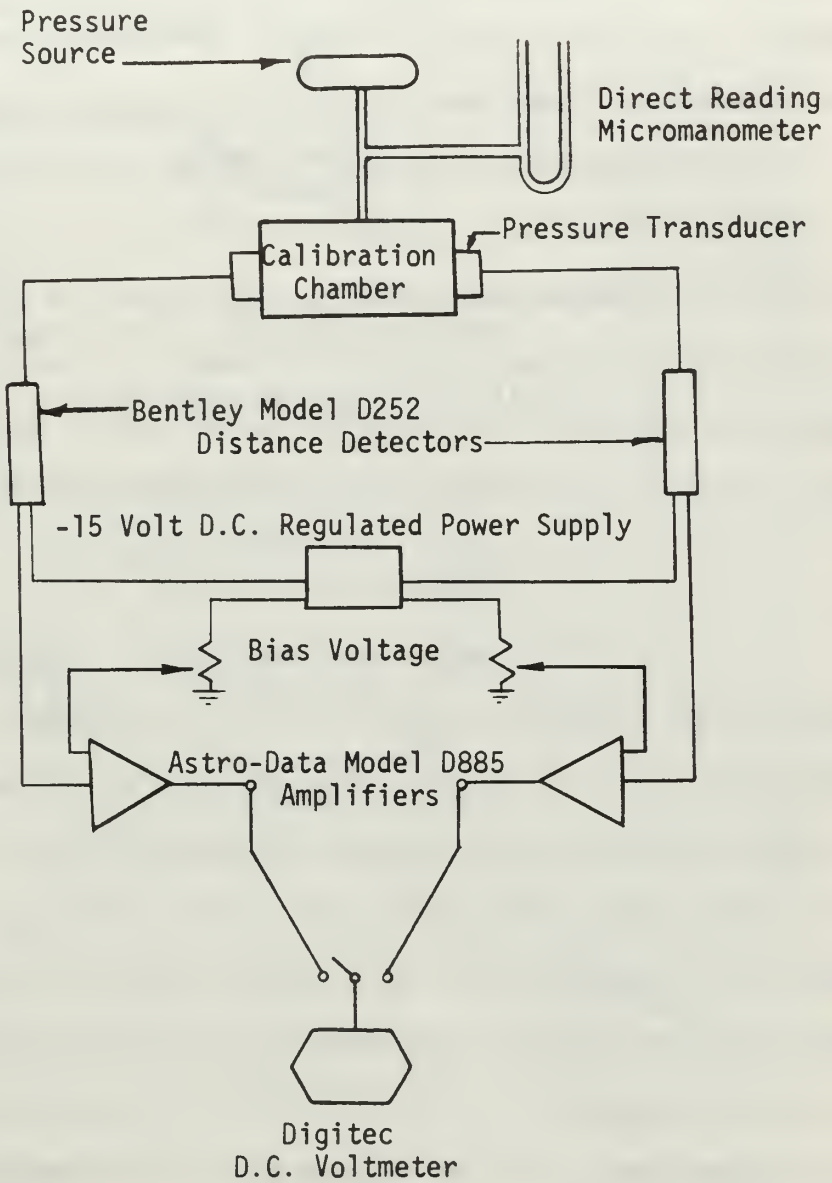

FIGURE 4 STATIC CALIBRATION INSTRUMENTATION

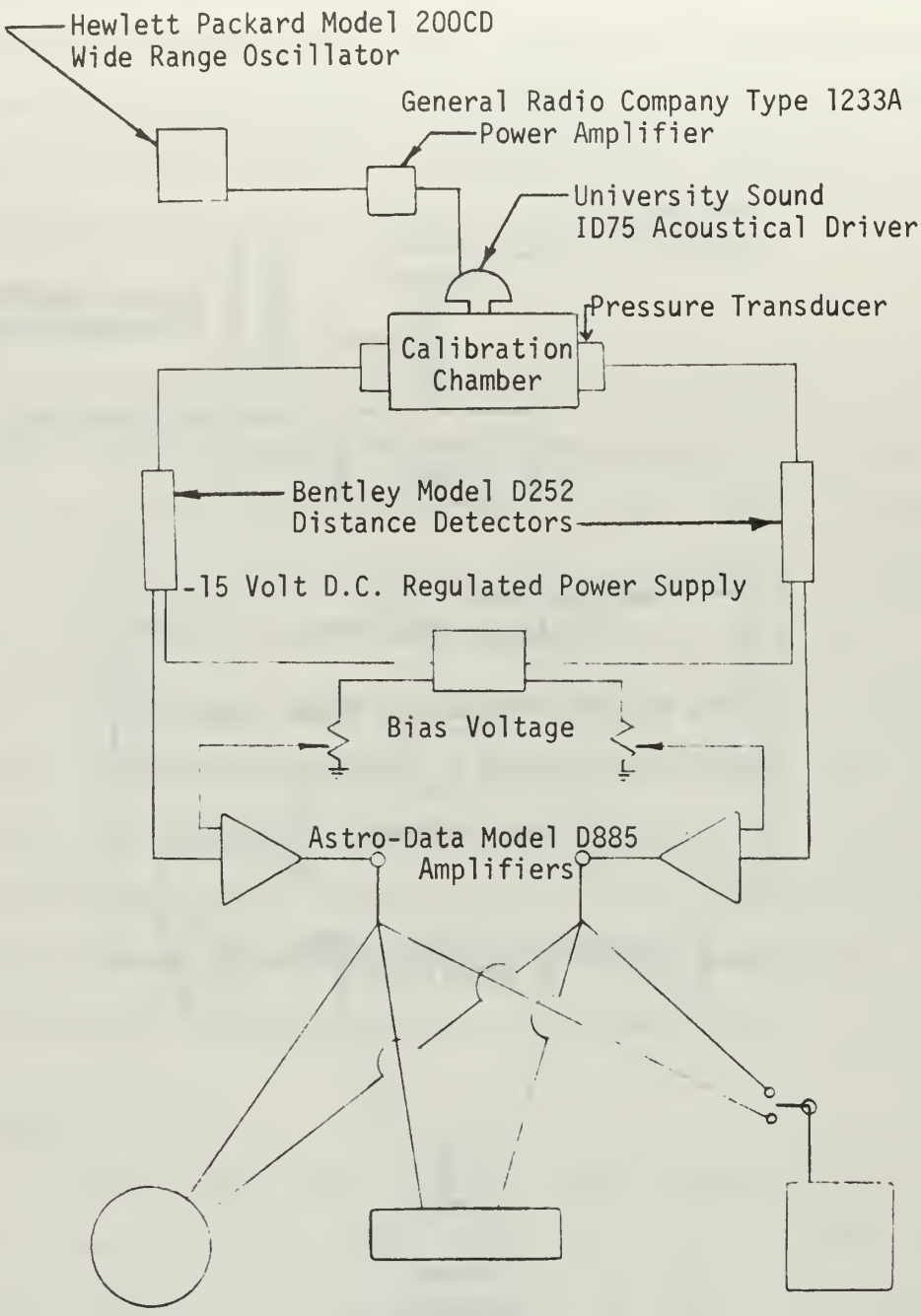

FIGURE 5 DYNAMIC CALIBRATION INSTRUMENTATION

position). These taps were connected to the pressure transducers with flexible Tygon tubing. The tubing used was a soft plastic with a 0.0465 inch inside diameter and a 0.125 inch outside diameter and had been previously calibrated relative to its unsteady pressure frequency response traits. The airfoil section is shown in Figure 6. Figures 7 through 10 are photographs of the wind-tunnel model employing the pressure measuring system. The plain flap was of light weight balsa construction glued to a 0.125 inch diameter steel drill rod. The deflection angle was sensed by a potentiometer located at the left-hand end of the model. A small steel tab installed in the center of the trailing edge of the flap and connected to a constant speed motor with steel piano wire provided actuation of the flap for dynamic tests.

II. CALIBRATION PROCEDURES

Static Calibration

Static response of the two pressure transducers used in this study was determined by installing the transducers in the calibration chamber, applying a known pressure, measured with a direct reading micromanometer, to the chamber and measuring the output voltage. The air gap between the sensing head and the brass diaphragm in the transducer was adjusted during this procedure to obtain a transducer output of 0.28 volts per p.s.i. which was linear in the pressure range of plus or minus 1.2 pounds per square inch gage (p.s.i.g.). A pressure change of 1.0 p.s.i. deflected the diaphragm approximately 0.00065 inches which corresponds to a deflection of less than one third the diaphragm thickness for the desired full pressure range. It was felt that an upper limit of one third the diaphragm thickness was the maximum deflection allowable in order to maintain a linear pressure calibration.

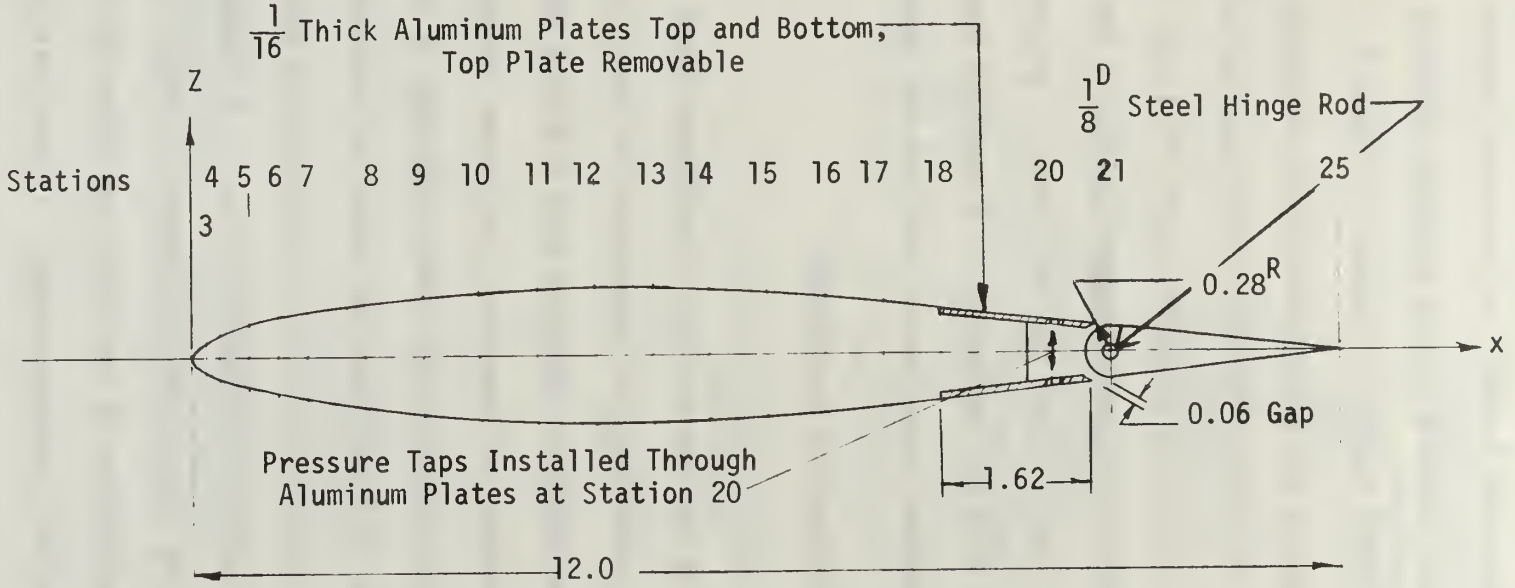

NOTES

1. All Dimensions in Inches
2. X-Z Coordinates Corresponding to Stations are Tabulated in Appendix C
3. Material: Main Airfoil - Mahogany
   Flap - Balsa

FIGURE 6 MODIFIED NACA 64_1-012 AIRFOIL WITH 20 PER CENT CHORD FLAP USED IN WIND TUNNEL TESTS

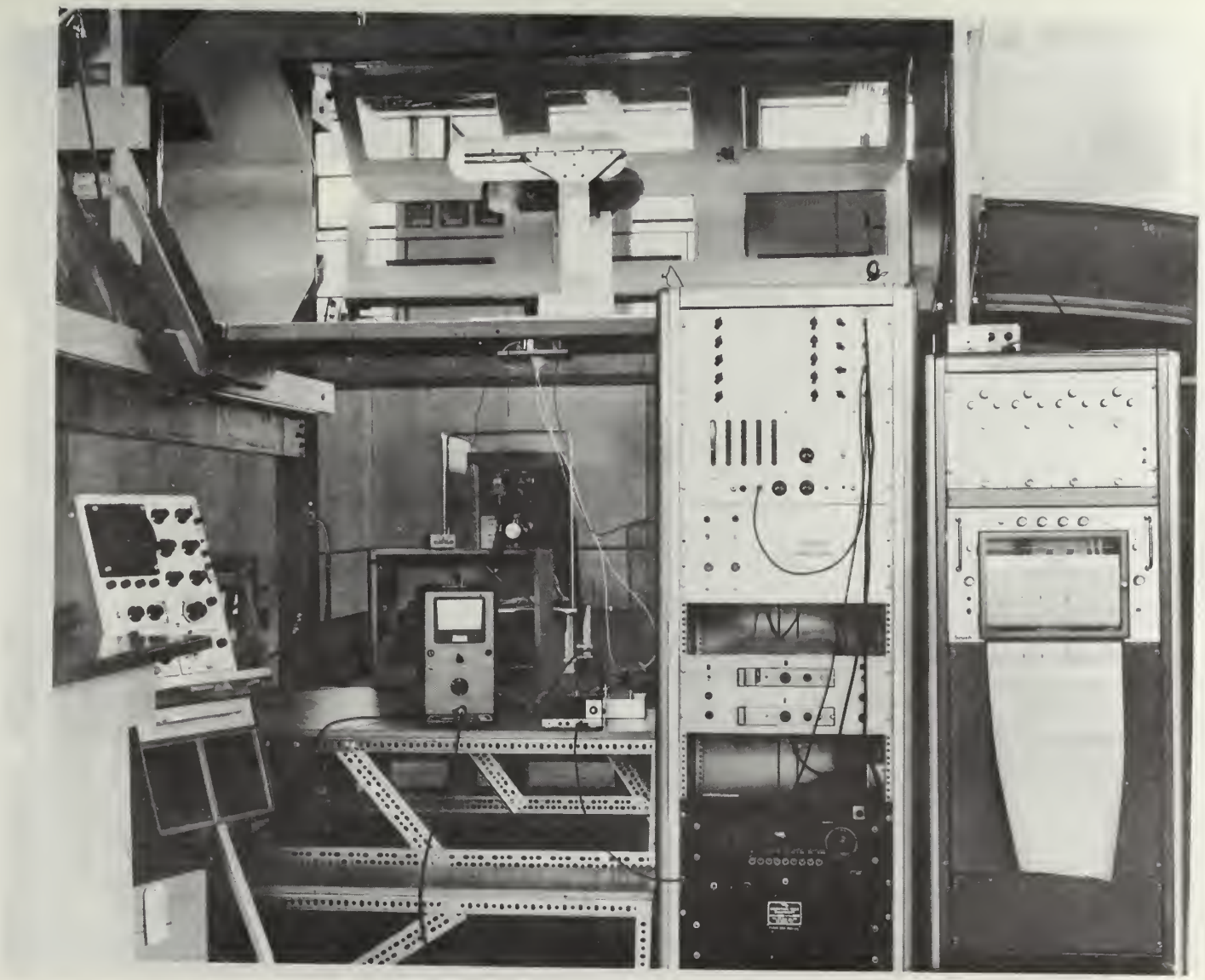

FIGURE 7 WIND TUNNEL APPARATUS

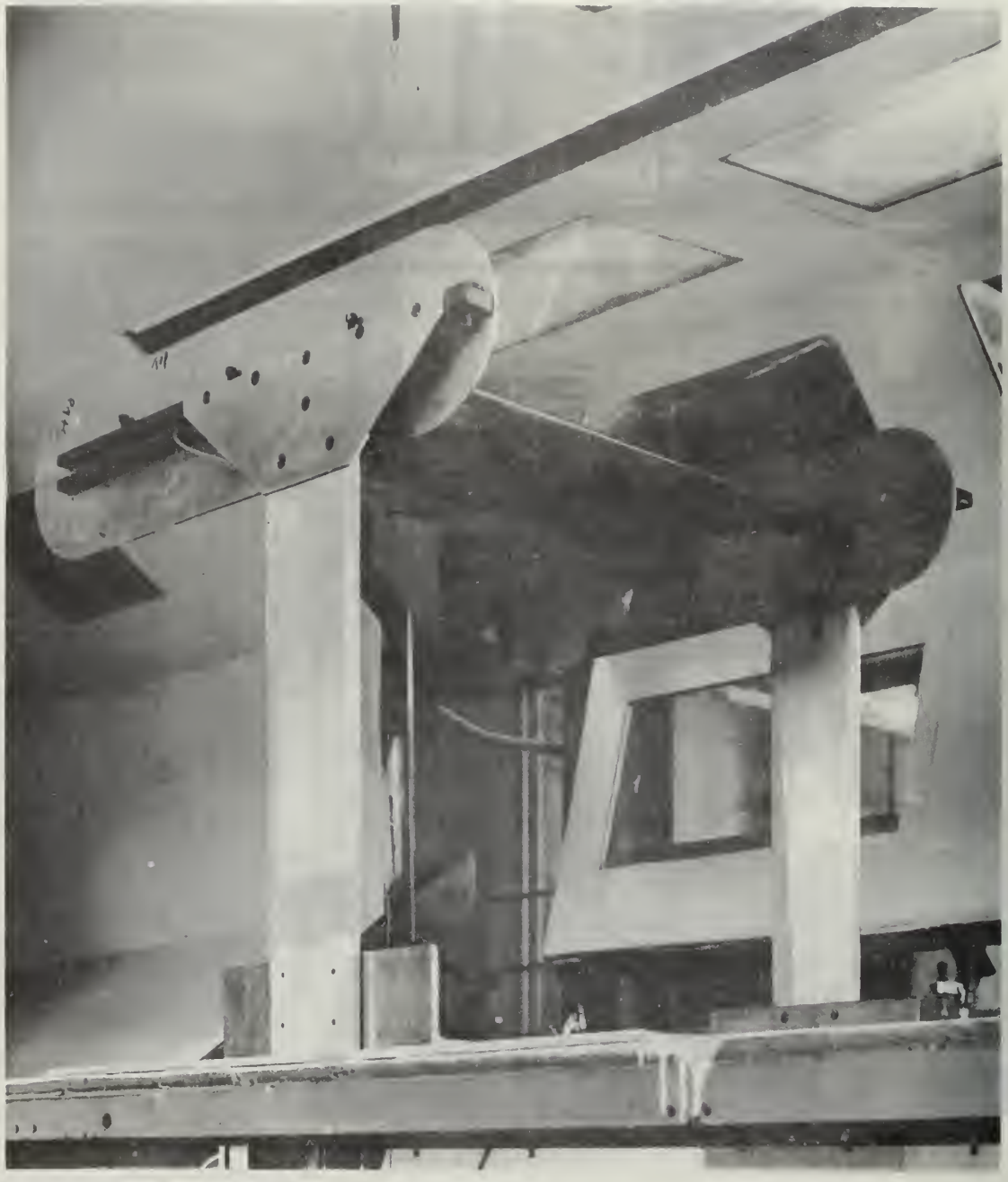

FIGURE 8 WIND TUNNEL MODEL

FIGURE 9 WIND TUNNEL MODEL SHOWING FLAP ANGLE OF ATTACK INDICATOR AND ACTUATOR

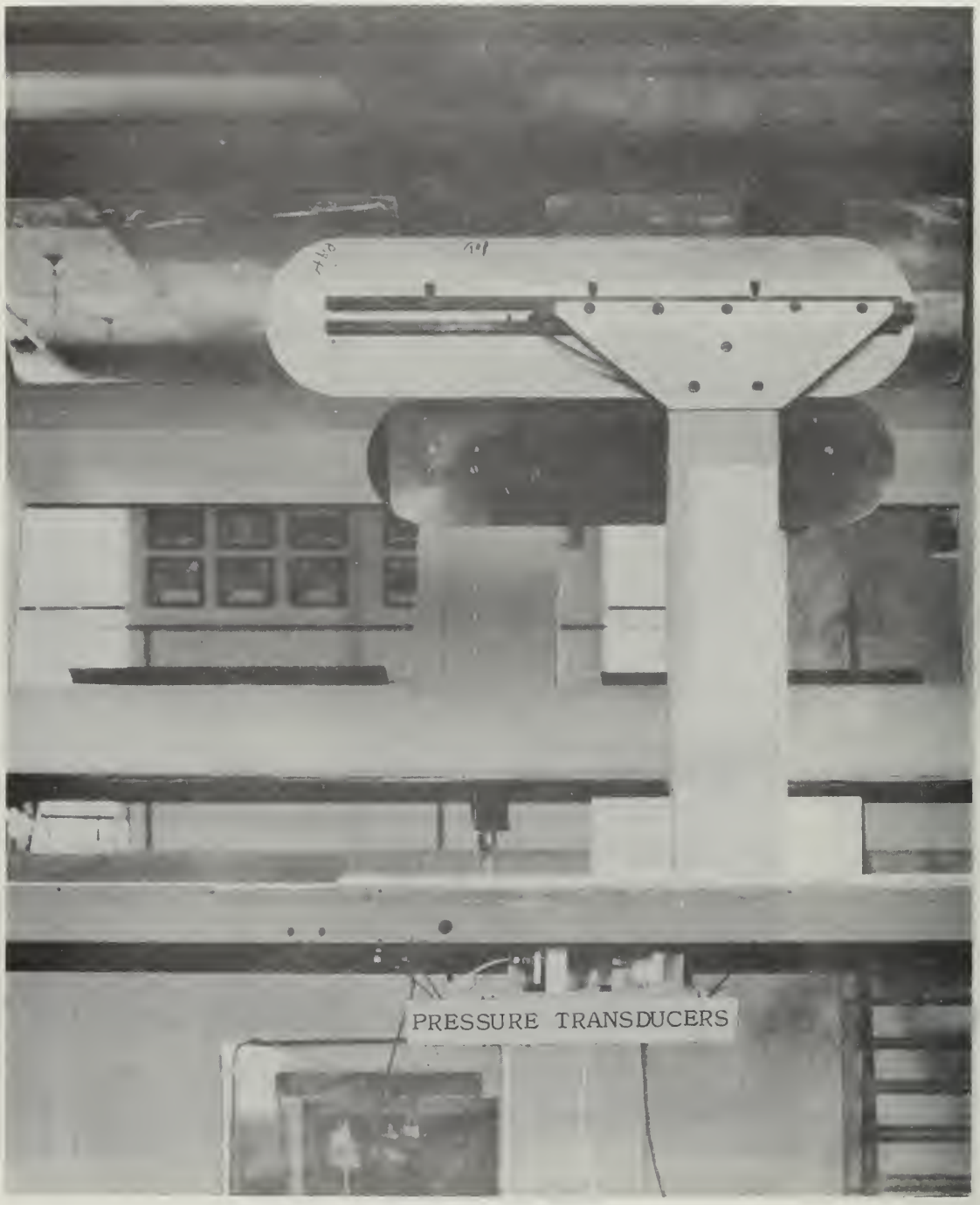

FIGURE 10 WIND TUNNEL MODEL WITH PRESSURE TRANSDUCERS MOUNTED BELOW THE WIND TUNNEL FLOOR

To obtain the dynamic characteristics of the pressure transducers and the proposed measuring system, the installation shown in Figure 5 was used. The initial runs were conducted with both transducers mounted in the calibration chamber. This configuration allowed a comparison to be made of the characteristics of the two transducers. The symmetry of the acoustical wave propagation was also verified by this test.

In order to obtain the dynamic response of the system to a remote pressure pickup, one transducer was connected to the calibration chamber by a flexible plastic tube as described above. Two different diameters of tubing were used, and the cavity volume which is formed in front of the transducer diaphragm face was varied, using ringlike spacers of varying thickness.

For dynamic calibration runs a fluctuating chamber pressure was produced by the acoustical driver unit. The values of phase difference and the R.M.S. value of pressure for both transducers were recorded at frequency increments of 5 Hertz from 10 to 400 Hertz.

Using the data recorded in each run a system dynamic gain, defined as P_2/P_1, was calculated. The values of calculated gain and measured phase angle were then plotted as a function of frequency to give a calibration curve for the system.

CHAPTER III

RESULTS AND DISCUSSION

Static Calibration

Figure 11 is the measured static calibration curve for the pressure transducer. The transducer output was amplified by a factor of ten, and the voltage output as a function of pressure was plotted to give a calibration curve. The curve was linear in the range plus or minus 1.0 p.s.i.g. This curve was checked repeatedly during a period of three months, and the variation was less than one per cent.

Dynamic Calibration

Dynamic calibration began by checking the dynamic response of the two transducers when subjected to the same fluctuating pressure. It was found that both systems had identical responses from 0 to 2500 hertz with the exception of some erratic behavior with respect to pressure signal wave form between 1500 and 2000 hertz, but this frequency range is near the resonant frequency of the calibration chamber cavity which, for standard atmospheric conditions, is given by:

$$\omega \text{ resonance} = \frac{a_o}{(\text{twice the cavity length})} \quad , \tag{1}$$

and equals 1835 hertz.

The harmonically varying pressure at the input end of a tube is given by:

$$\bar{P}_1 = P_o + P_1 e^{i\omega t} \quad , \tag{2}$$

and at the tube exit into the transducer cavity volume is:

$$\bar{P}_2 = P_o + P_2 e^{i(\omega t - \theta)} \quad . \tag{3}$$

Therefore, the dynamic characteristics of the pressure measuring system are defined by the amplitude ratio, $\frac{P_2}{P_1}$, and the relative phase shift, θ.

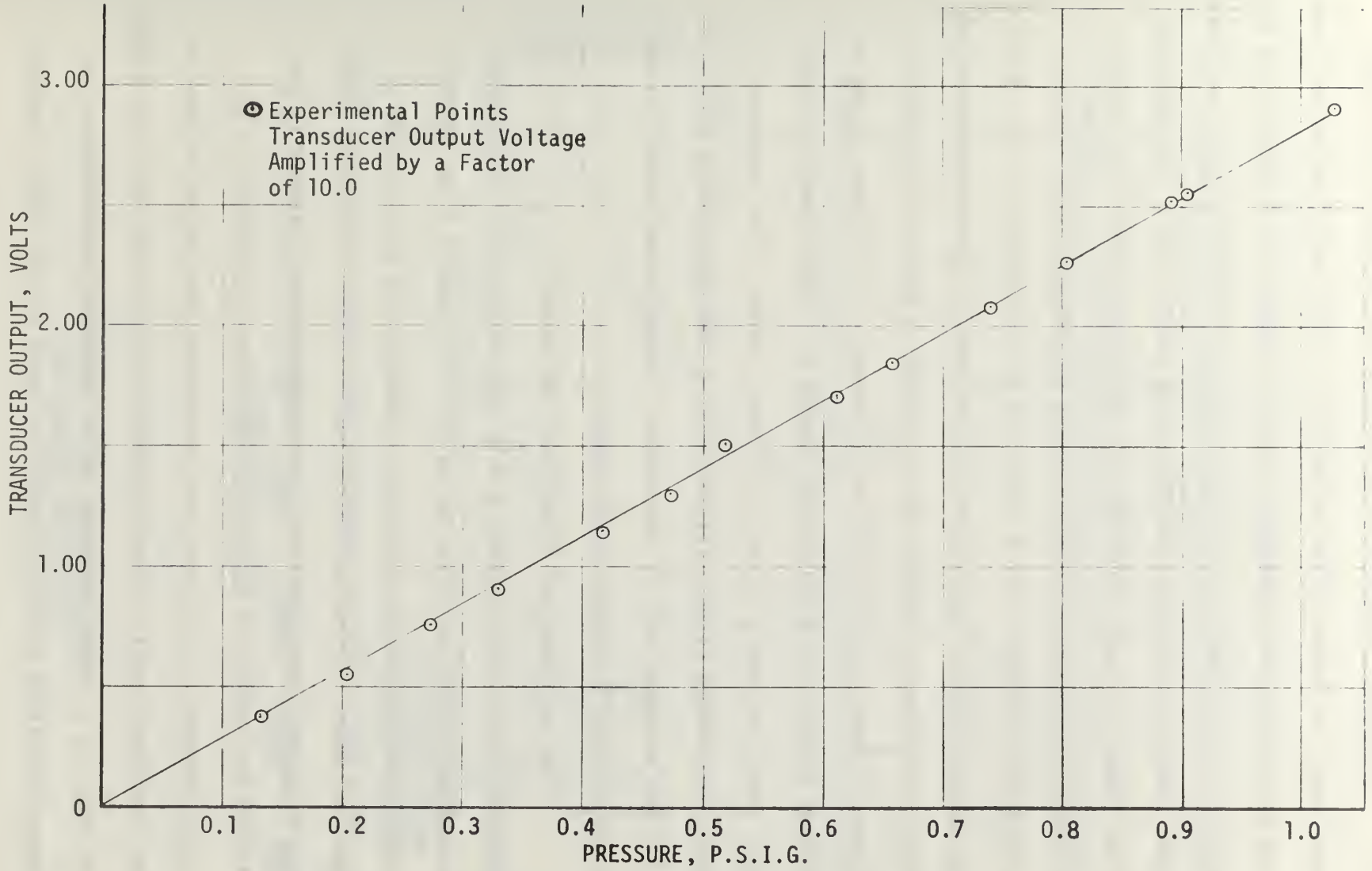

FIGURE 11 PRESSURE TRANSDUCER STATIC CALIBRATION CURVE

In order to determine the effects of very short rigid pressure lines, an adapter plate containing a 0.020 inch diameter hole was used to separate one transducer from the chamber. The adapter had shim inserts which allowed the distance that the transducer cavity was separated from the calibration chamber to be varied from 0.188 inches to 0.288 inches. It was found that the oscillatory signal was transmitted to the remote transducer almost unattenuated from 0 to approximately 100 hertz with a phase lag of 6.0 degrees or less, with the measured signal lagging the applied signal. This result confirms results obtained by Schmidt [4] and stated by Berg and Tijdeman [3]. Figure 12 shows a typical plot of $\frac{P_2}{P_1}$ versus ω. This case is for an orifice diameter of 0.020 inches, length of 0.288 inches and transducer cavity volume of 1.454×10^{-2} cubic inches. The transducer cavity was formed using a Teflon washer 0.038 inches thick with a 0.60 inch diameter hole in the center. Other volumes were obtained by varying the thickness of the washer.

The next phase of determining the behavior of oscillatory pressure transmission through a thin tube consisted of moving the second transducer away from the calibration chamber to an external holder connected to the calibration chamber by a plastic tube as described above. Three parameters were studied during this phase: tube diameter, tube length and transducer volume. Figures 13 and 14 show the effects of varying the individual parameters on the system response. It is seen that increasing the length of tube or the transducer cavity volume decreases the amplitude ratio and shifts the peaks to a lower frequency, while increasing tube diameter increases amplitude ratio and moves the peaks to the higher frequency.

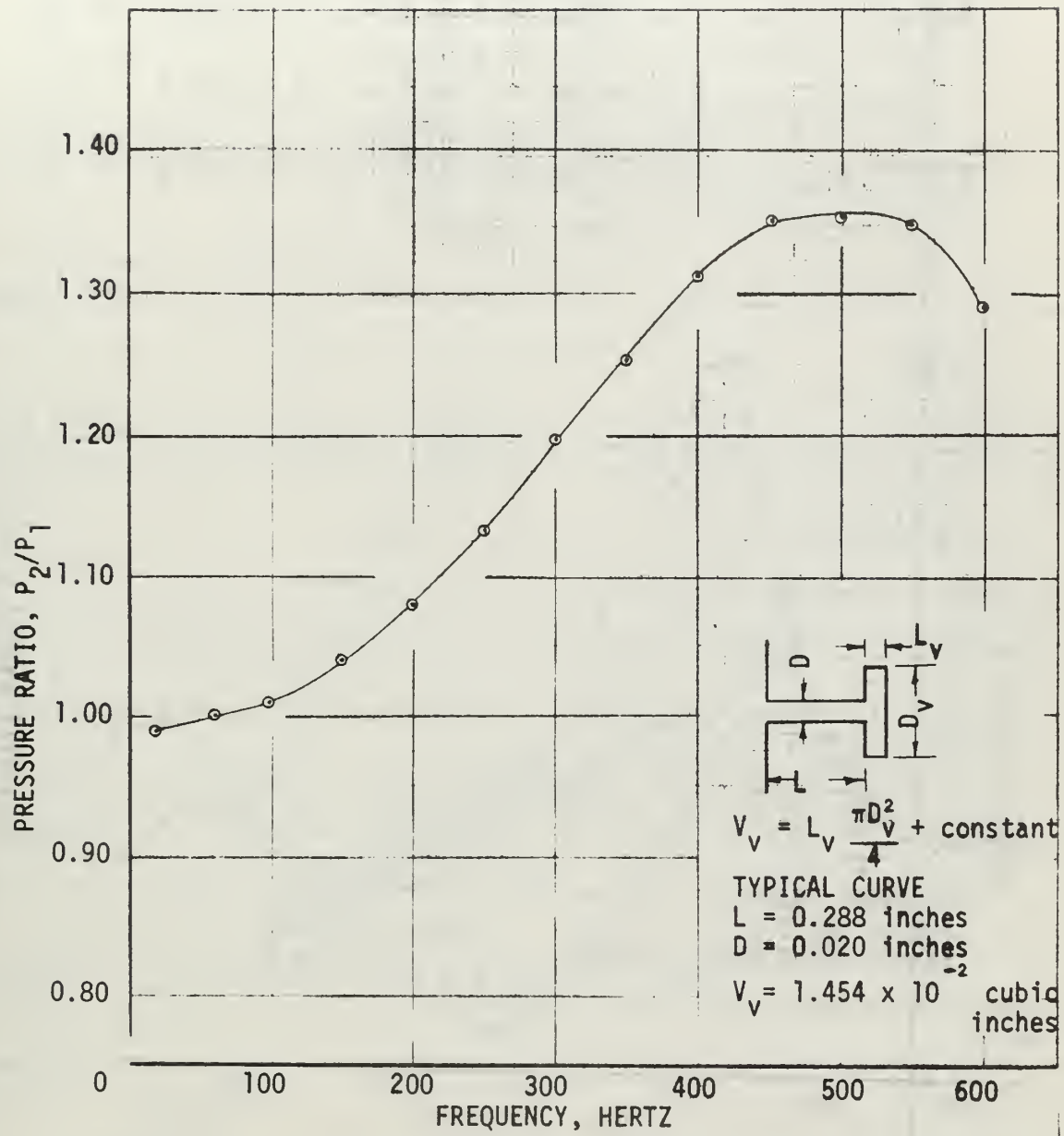

FIGURE 12 PRESSURE RATIO VERSUS FREQUENCY FOR A SHORT RIGID TUBE

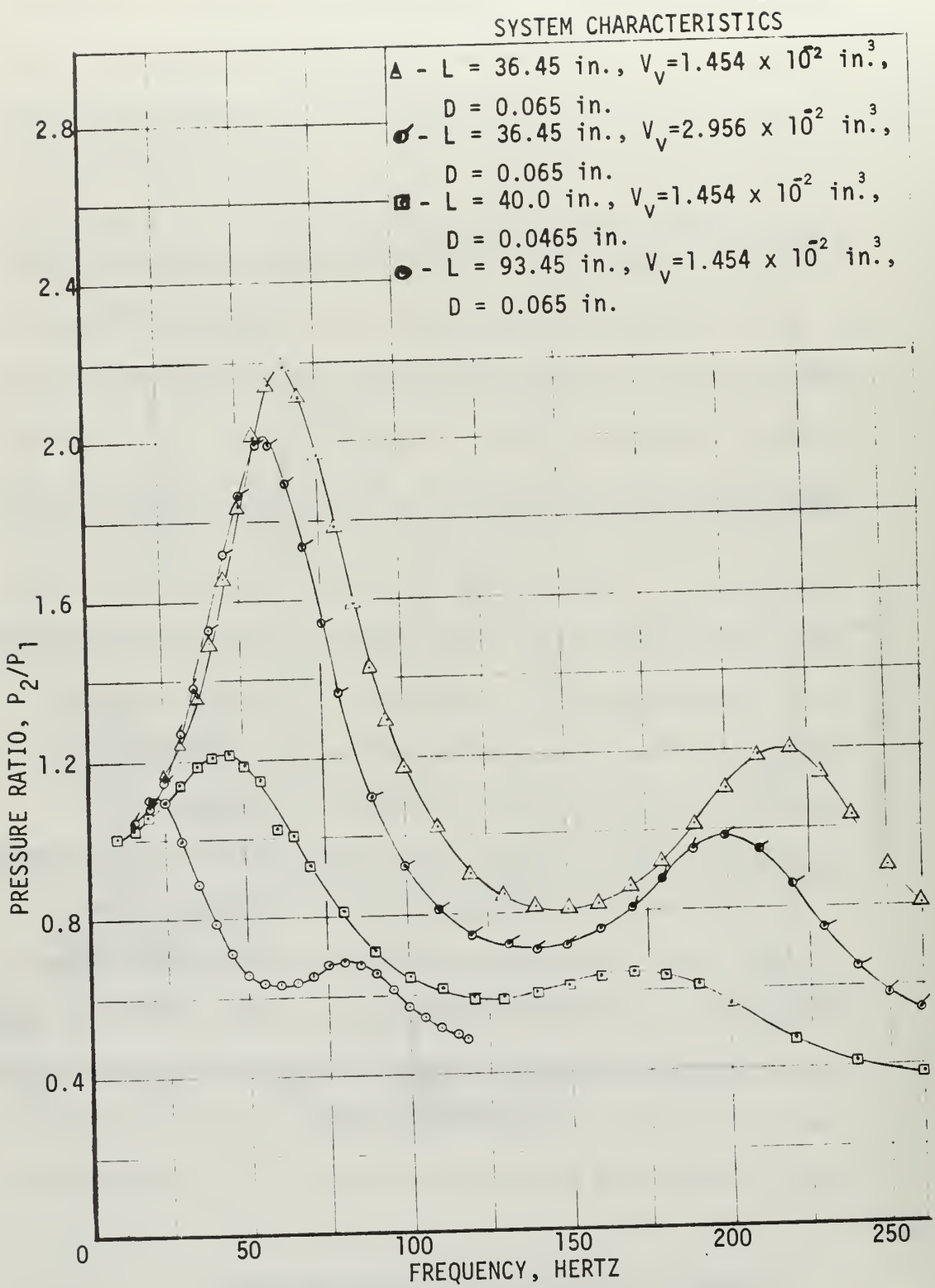

FIGURE 13 EFFECT OF SYSTEM GEOMETRY ON PRESSURE RESPONSE

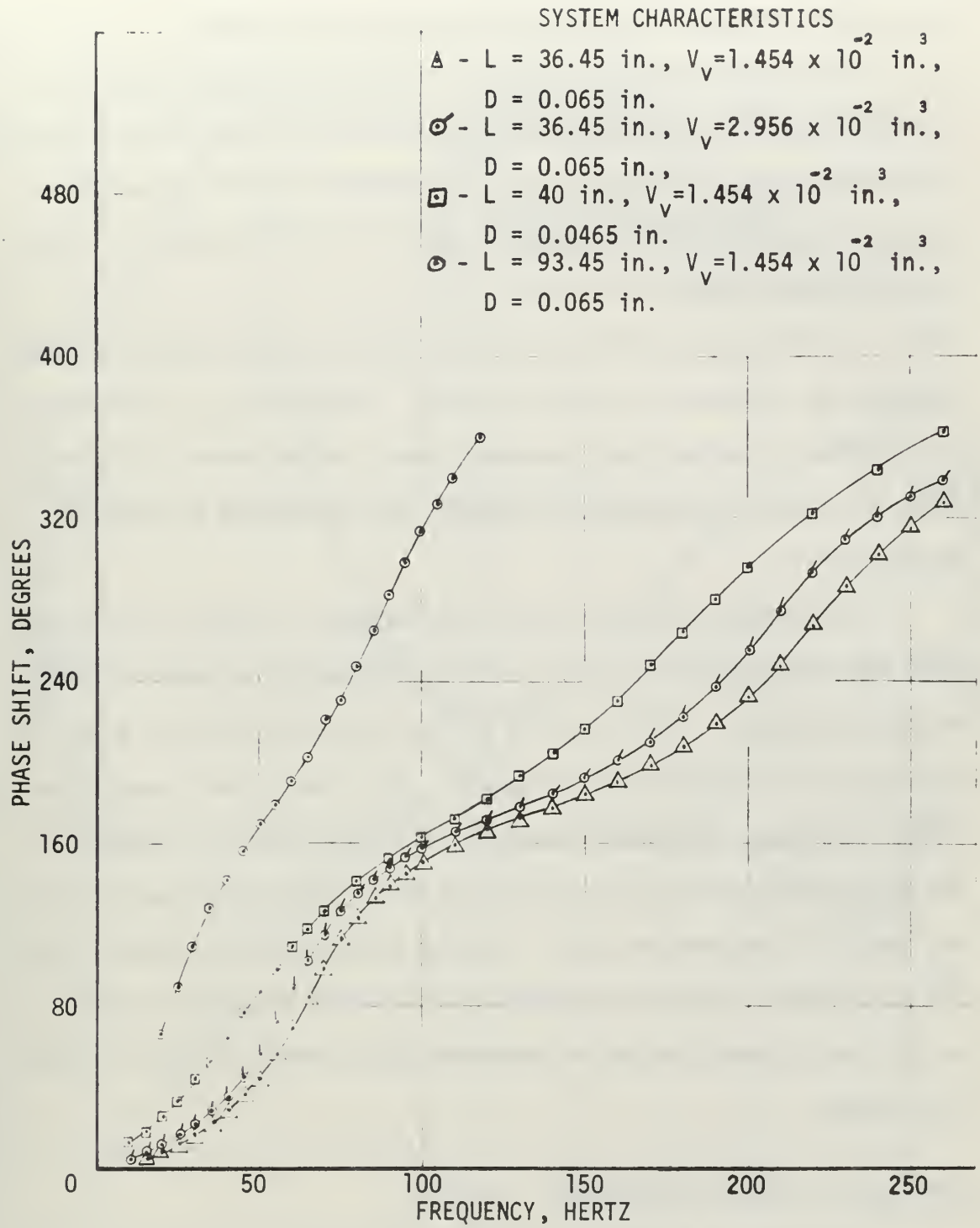

FIGURE 14 EFFECT OF SYSTEM GEOMETRY ON PHASE SHIFT

The relative phase shift was only slightly changed by varying cavity volume and tube radius, but a much greater phase shift was measured for a given frequency when the tube length was increased.

The removal of the transducer from the calibration chamber and its installation in an external holder now simulates the working system. The unsteady pressure signal is now transmitted from the source (the calibration chamber) to the measuring device (the transducer) through the thin plastic tube.

In choosing a working system it was felt that a smooth transfer function was necessary for practical use. Therefore, if a combination of parameters produced sharp resonance peaks during dynamic calibration, the system, although well defined, was considered an unusable configuration.

One approach that was used in an attempt to smooth out resonance was the placing of a tee in the line between the pressure source and the transducer. The third leg of the tee was fitted with a tube which was to act as an acoustic damper. This idea proved unusable as sharper resonance peaks were developed no matter what the length of the damping tube, which was varied from 10 per cent to 100 per cent of the length of the pressure lead. An even more disturbing effect from the system with a tee was the erratic phase shift produced, possibly due to the different values of resonance associated with the different tube lengths.

Wind Tunnel System Calibration

The pressure measuring system chosen for use in the wind tunnel was composed of 40 inches of 0.0465 inch inside diameter plastic tubing connected to a transducer volume of 2.965×10^{-2} cubic inches. The calibration curve for this system is shown in Figure 15.

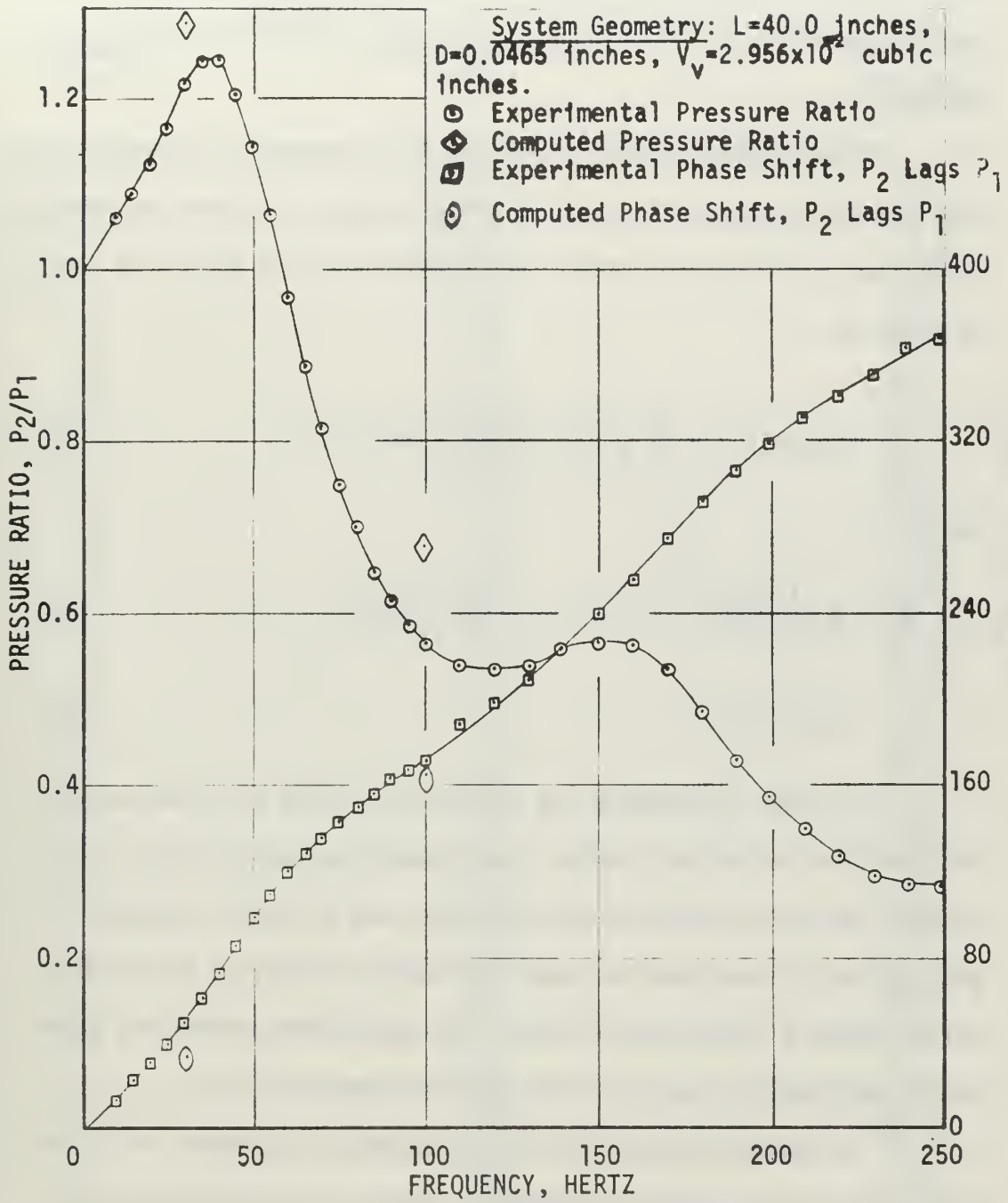

FIGURE 15 DYNAMIC RESPONSE TRAITS OF FINAL MEASURING SYSTEM CONFIGURATION

Repeatability of the calibration run was found to be good, as the variation during runs was less than one per cent. Table I summarizes the experimental calibration values of phase angle and amplitude ratio for each frequency that generated the calibration curve applicable to the configuration used in the wind-tunnel measuring system.

A theoretical model to predict the response of a remote pressure measuring system to an oscillating pressure has been proposed by Bergh [1,2]. In Bergh's model (See Appendix A) the amplitude ratio is given by:

$$\frac{P_2}{P_1} = \left[\cosh(\phi L) + \frac{\omega^2}{a_o^2} \frac{\gamma}{k} \frac{V_v}{V_t} \frac{L}{\phi} \frac{J_o(\alpha)}{J_2(\alpha)} \sinh(\phi L)\right]^{-1} \tag{4}$$

where

$$\phi = \frac{\omega}{a_o} \left(\frac{J_o(\alpha)}{J_2(\alpha)}\right)^{\frac{1}{2}} \gamma^{\frac{1}{2}} \left[1 + \frac{\gamma-1}{\gamma} \frac{J_2(\alpha P_r^{\frac{1}{2}})}{J_o(\alpha P_r^{\frac{1}{2}})}\right]^{\frac{1}{2}} \tag{5}$$

$$\alpha = i^{\frac{3}{2}} R \left(\frac{\rho_o \omega}{\mu}\right)^{\frac{1}{2}} . \tag{6}$$

In order to compare the theoretical model with the curves obtained for the actual system, two theoretical points were calculated. The calculations were laborious, and a digital computer program would have been desirable for calculating more points and establishing a theoretical curve. The calculated points are shown on the calibration curve for the system (symbols ◇, 0).

The calculated points are in reasonable agreement with the calibration curve. The discrepancies which are present may be attributed mainly to the uncertainties in the measured physical properties of the system. The small diameters and thickness which must

TABLE I

DYNAMIC CALIBRATION DATA FOR PRESSURE MEASURING SYSTEM WITH

L = 40 inches $V_v = 2.956 \times 10^{-2}$ cubic inches

D = 0.0465 inches

Frequency (Hertz)	Pressure Ratio (P_2/P_1)	Phase Shift (degrees) P_2 lags P_1
10	1.06	14.5
15	1.09	22.5
20	1.125	31.0
25	1.163	40.0
30	1.219	49.5
35	1.244	61.5
40	1.244	73.5
45	1.203	86.5
50	1.144	99.0
55	1.063	109.5
60	0.969	102.0
65	.888	128.0
70	.813	136.0
75	.750	143.0
80	.700	149.5
85	.650	156.0
90	.613	162.0
95	.588	167.0
100	.566	171.0
100	.565	171.0
110	.540	189.0
120	.535	198.0
130	.540	209.0
140	.560	223.0
150	.565	238.0
160	.563	255.0
170	.535	275.0
180	.485	291.0
190	.430	306.0
200	.385	319.0
210	.348	330.0
220	.318	341.0
230	.295	351.0
240	.285	364.0
250	.280	367.5
260	.278	378.0
270	.278	389.0
280	.280	403.0
290	0.280	417.0

be measured could easily lead to inaccuracies in calculated data. For example, the inside diameter of the plastic tubing could only be measured using a wire drill as a plug gage. This at best gave a rough mean inside diameter. The thickness of the Teflon used to produce the transducer volumes was found to vary in thickness by three to four thousandths of an inch. Thus the thickness was a mean value.

Bergh and Tijdeman [3] present a number of calibration curves for various pressure measuring systems. Although no attempt was made to exactly duplicate any one of the systems investigated by Bergh and Tijdeman, the same qualitative system responses were noted in this study. In the present study the purpose was to prove experimentally that a workable pressure sensing system could be constructed and calibrated with a high degree of reliability. That the system was reliable is demonstrated by the fact that during the experiments both the static and dynamic calibration curves were frequently checked and found to vary less than one per cent.

In order to extend the system capability to measure random pressure fluctuations the indicial response of the system was measured. The calibration chamber pressure was abruptly changed from one p.s.i.g. to atmospheric, and the system response was displayed on an oscilliscope. It was found that the system time constant, τ, where:

$$\tau = \Delta t \text{ (for pressure drop from } P_1 \text{ to atmospheric)}, \qquad (7)$$

was thirteen milliseconds with the transducer installed directly in the calibration chamber and fourteen milliseconds with the transducer connected to the chamber by a 40.0 inch tube, demonstrating that the effect of the connecting tube on system response is indeed small. A "dime store" balloon connected to the calibration chamber through a

0.25 inch diameter tube was exploded in order to produce the abrupt pressure change.

An Application of the Pressure Measuring System

Once a dynamic calibration curve had been obtained, the measuring system was integrated into the wind-tunnel model.

A zero frequency measurement was performed to determine the slope of the static pressure coefficient between the top and bottom surface per degree of control surface deflection. The pressure coefficient is given by:

$$\Delta Cp = \frac{P_L - P_u}{q} . \qquad (8)$$

The position of the pressure taps on the airfoil were at the 75 per cent chord position which was 5 per cent chord ahead of the control surface hinge line. To verify that the static pressure measurement was correct, pressure taps similar to those connected to the pressure transducers were installed at the same chord location and connected to a manometer board. The pressure change across the airfoil measured in this manner was found to be the same as that measured by the pressure transducers. The value of the slope of the static pressure coefficient curve per degree of flap deflection was found to be

$$\left(\frac{d\Delta Cp}{d\delta}\right)_{static} = 0.047 \text{ per degree.}$$

Thin airfoil theory, Appendix B, indicates a value for this coefficient of 0.059 per degree, which is larger than that actually obtained. Etkin [5], however, discloses that thickness ratio has an effect upon the hinge moments of a flapped airfoil, and it would be expected that the static pressures near the hinge line of the control surface would be similarly affected. The hinge moment value given in

[5] for a 12 per cent thick airfoil is 83.5 per cent of the zero thickness value. If this correction were applied to the calculated slope of the pressure coefficient, the value would become 0.049 per degree which agrees well with the measured value.

In order to determine the effect of control surface gap on the static pressure readings, a zero frequency test was conducted for varying surface deflections with the gap completely sealed. The static pressures obtained during this test were identical to those obtained with the gap unsealed, and it can be assumed there was little or no flow leakage through the control surface gap.

Due to mechanical limitations it was possible to run at only a single frequency to check the dynamic characteristics of the pressure measuring system. The control surface was oscillated at 28.5 hertz using a constant speed electric motor. This limitation of a single frequency would be a deficiency in an experiment if the goal were other than the operational proof of the system. The R.M.S. values of control surface deflection and upper and lower surface pressures were recorded for eight runs with a tunnel dynamic pressure of 24.18 pounds per square foot. The measured pressures were corrected for transducer system dynamic gain according to Figure 15, the amplitude ratio, $\frac{P_2}{P_1}$, for 28.5 hertz being equal to 1.20. Using the data obtained, a dynamic value for the pressure difference across the wing was determined. The average value of the slope of the pressure coefficient per degree was

$$\frac{d\Delta C_p}{d\delta}_{\text{dynamic}} = 0.045 \text{ per degree.}$$

Figure 16 is a simultaneous recording made of the output of both pressure transducers and the control surface position on a Brush Instruments

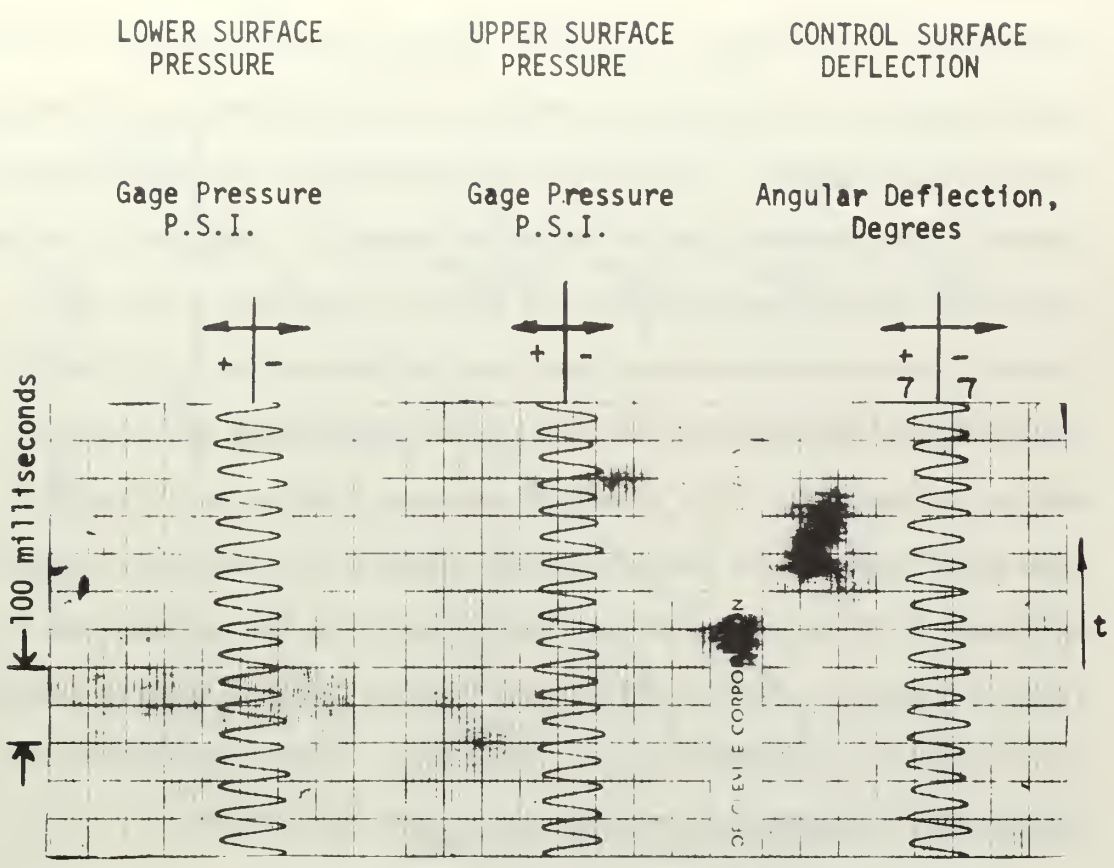

The following R.M.S. values of pressure and control surface deflection were recorded with tunnel dynamic pressure, q, equal to 24.18 pounds per square foot and flap frequency, ω, equal to 28.5 Hertz.

Lower Surface Pressure = 0.020 p.s.i.g.
Upper Surface Pressure = 0.020 p.s.i.g.
Control Surface Deflection = 4.99 degrees

FIGURE 16 OSCILLOGRAPH RECORDING OF FLAP DEFLECTION AND PRESSURE OSCILLATION ON THE AIRFOIL SURFACE

Ultralinear Oscillograph. From left to right the traces are of pressure fluctuation on the lower surface, the upper surface, and control surface displacement. The traces are annotated to indicate maximum control surface travel, which was approximately 7.0 degrees in either direction, and maximum positive and negative pressures. The oscillograph traces were used as a check on the measured oscillation frequency and to monitor the behavior of the transducers and control surface driver unit. The values of pressure used in obtaining pressure coefficients were those obtained from R.M.S. readings. Kussner and Schwarz [6] present a method for determining the pressure coefficient across an airfoil with an oscillating plain flap (See Appendix B). The pressure coefficient is shown to be a function of the non-dimensional frequency, k, of the airfoil and is given by:

$$\Delta Cp(\beta,t) = \frac{4}{\pi}\,\delta\, e^{i\omega t}[Re(k,\beta,\psi) + iIm(k,\beta,\psi)] \qquad (9)$$

where

$$\cos\beta = -x/c\ . \qquad (10)$$

This equation comes from the paper by Kussner and Schwarz [6], may also be found in Fung [7], and is more completely defined in Appendix B. The results of this equation are shown on Figure 17, where the pressure attenuation and phase angle are plotted versus non-dimensional frequency, k, for a value of β corresponding to the 75 per cent chord position when the plain flap hinge line is at the 80 per cent chord position. The value of non-dimensional frequency which corresponds to the measured wind tunnel data is 0.77, which gives a pressure attenuation of 0.93. Using the value of the slope of the static pressure coefficient curve calculated from thin airfoil theory and corrected for finite thickness and applying the attenuation factor of 0.93, the

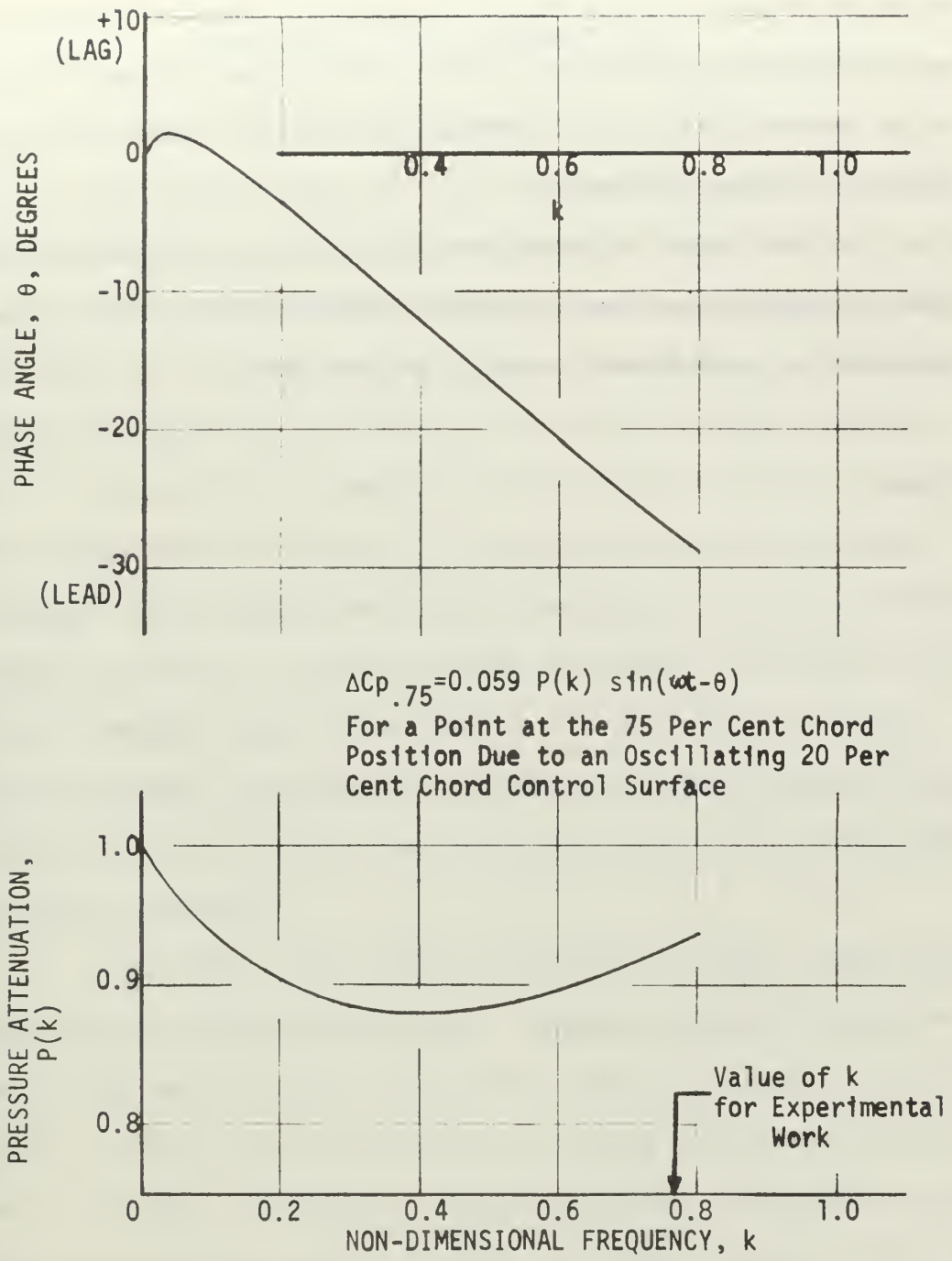

FIGURE 17 PRESSURE ATTENUATION AND PHASE ANGLE VERSUS NON-DIMENSIONAL FREQUENCY

calculated value of the slope of the dynamic curve becomes 0.046 per degree which agrees well with the experimental results. The pressure peak at the 75 per cent chord position should lead the peak flap oscillation theoretically by 27.5 degrees. No attempt, however, was made to measure this phase difference.

A final check on the system calibration was performed when the work in the wind tunnel was complete. The calibration curve, Figure 15, was found to be confirmed to within one per cent.

CHAPTER IV

CONCLUSIONS AND RECOMMENDATIONS

I. CONCLUSIONS

Calibration showed the static and dynamic properties of the pressure transducer system very well behaved. Both steady and unsteady static pressures were easily measured, and the measurements were repeatable to a high degree of accuracy. The correlation between theory and experiment could have been better, but precise measurements of the physical parameters were difficult to obtain. Indeed, for a large number of tubes in an installation employing only one transducer and a scanner valve type arrangement, it would be advantageous to install a second transducer internally to the model. This second transducer would allow more flexibility in the use of the measuring system. A continuous calibration of the system would be available by simultaneously measuring the pressure at a given station with both transducers.

The system is very easily installed in a model. Weight and cost wise the advantages are great. Unsteady pressure loads on an oscillating model are easily obtained without the necessity of correcting readings for the acceleration response of the individually mounted internal transducers. For these reasons, the system would be good for determining dynamic loadings for flutter analysis without the need to build an elaborate dynamic model with many small and costly model installed transducers.

The experimental results obtained during the wind tunnel tests compare well with those obtained using thin airfoil theory.

Use of this method of unsteady pressure measurements is not limited to cases of purely harmonic flow. The calibration curve generated for the measuring system is in essence a system transfer function. With the transfer function known, the measuring technique may be used to measure stochastic pressure variations such as those encountered in regions of separated flow. For this type application, instead of measuring the transducer output directly, a recording of the transducer output could be made on magnetic tape and a power spectral analysis performed on the recorded signal to determine the character of the random pressure variation.

II. RECOMMENDATIONS

Pressure measuring systems of this type have not been used before at the Naval Postgraduate School. Neither have they been used, as far as it is known, to any great extent in this country. The system constructed for this study has proven practical but could be improved upon in a number of ways.

In the area of transducer construction a smaller sensing head could be utilized to construct a smaller transducer. The instrumentation setup seems to be sound, but some transient high frequency noise, although only in the 2.0 to 3.0 millivolt range, was a bother and could be eliminated with some work on the circuit wiring.

Bergh's [1] theoretical analysis appears accurate. If a digital computer program were written to use this analysis in a parametric study of the physical variables, it might be much faster to choose a suitable combination of these variables to fit a particular application.

This measuring system should be integrated into a larger and more complex model in conjunction with a multi-channeled scanning valve arrangement, to explore the full capability it seems to have.

REFERENCES

1. Bergh, H., "A New Method for Measuring the Pressure Distribution on Harmonically Oscillating Wings," Proceedings of the 4th ICAS Congress, Paris, 1964.

2. Lashka, B., Die Druck-, Auftriebs- und Momentenverteilungen an einem harmonisch schwingenden Pfeilflugel Kleiner Streckung im niedrigen Unterschallbereich. Vergleich zwischen Theorie und Messung," Proceedings of the 4th ICAS Congress, Paris, 1964.

3. Bergh, H., and H. Tijdeman, "Theoretical and Experimental Results for the Dynamic Response of Pressure Measuring Systems," NLR-TR F.238, National Aero- and Astronautical Research Institute, Amsterdam, 1965.

4. Schmidt, L. V., "Measurement of Fluctuating Air Loads on a Circular Cylinder," Ph.D. Thesis, California Institute of Technology, 1963.

5. Etkin, B., Dynamics of Flight, New York: John Wiley and Sons, Inc., 1959, Appendix B.

6. Kussner, H. G., and L. Schwarz, "The Oscillating Wing with Aerodynamically Balanced Elevator," N.A.C.A. Technical Memorandum Number 991, October, 1941.

7. Fung, Y. C., The Theory of Aeroelasticity, New York: John Wiley and Sons, Inc., 1955, Chapter 13.

APPENDIX A

THEORY FOR DYNAMIC RESPONSE OF A THIN TUBE TO OSCILLATING PRESSURE

The treatment presented here is due to Bergh [1] and is concerned with the solution for the pressure response into a transducer cavity when a long slender tube is used to connect the transducer cavity to the unsteady pressure source. No correction is made for tube wall elasticity as might be envisioned in a biological environment since it was experimentally confirmed that the difference in dynamic response between using a metal tube or a plastic tube was negligible for the configurations considered.

The unsteady terms are postulated as harmonic perturbations superimposed upon the mean average values in the following expressions for the dominant variables:

$$\begin{aligned}
&\text{Pressure:} && \bar{p} = p_o + p\, e^{i\omega t} \\
&\text{Density:} && \bar{\rho} = \rho_o + \rho\, e^{i\omega t} \\
&\text{Temperature:} && \bar{T} = T_o + T\, e^{i\omega t} \\
&\text{Axial Velocity:} && \bar{u} = u_o + u\, e^{i\omega t} \\
&\text{Radial Velocity:} && \bar{v} = v_o + v\, e^{i\omega t}
\end{aligned} \qquad \text{(A.01)}$$

The above terms are considered in the polar coordinate form due to the inherent symmetry about the tube axis. Typically, the pressure perturbation amplitude, p, in equation (A.01) would be functionally expressed as $p(x,r)$ where x is the axial distance from the input end of the tube and r represents the radial distance from the axis of tube symmetry. The four governing relations are the Navier-Stokes equations, the continuity equation, the equation of state for

an ideal gas, and the unsteady form of the energy equation. Under the assumptions that:

a. The disturbances are small,

b. The tube radius is small compared to its length, and

c. Laminar flow exists throughout the system,

the controlling equations may be linearized in terms of the perturbations to yield the following set of coupled partial differential equations:

$$-\frac{1}{\rho_o}\frac{\partial p}{\partial x} + \frac{\mu}{\rho_o}\left[\frac{\partial^2 u}{\partial r^2} + \frac{1}{r}\frac{\partial u}{\partial r}\right] = i\omega u \qquad (A.02)$$

$$\frac{\partial p}{\partial r} = 0 \qquad (A.03)$$

$$-\rho_o\left[\frac{\partial u}{\partial x} + \frac{\partial v}{\partial r} + \frac{v}{r}\right] = i\omega\rho \qquad (A.04)$$

$$\frac{\gamma}{a^2_o}\left[1 + \frac{\rho_o}{T_o}\frac{T}{\rho}\right] = \rho \qquad (A.05)$$

$$\lambda\left[\frac{\partial^2 T}{\partial r^2} + \frac{1}{r}\frac{\partial T}{\partial r}\right] - i\omega\rho = i\omega\rho_o g C_\rho T \ . \qquad (A.06)$$

These partial differential equations are subject to the following boundary conditions:

a. At the wall of the tube, $r = R$;

$u(x,R) = 0$, $v(x,R) = 0$, and $T(x,R) = 0$. (A.07a)

The latter boundary condition implies that the conductivity of the wall is assumed to be sufficiently large, therefore, the temperature variation at the wall may be neglected.

b. At the center of the tube, $r = 0$;

by symmetry conditions, $v(x,0) = 0$, and

$u(x,0)$, $T(x,0)$, $p(x,0)$, and $\rho(x,0)$ are finite. (A.07b)

Equation (A.03) implies that the pressure perturbation is a function of axial distance x only. The energy equations may be treated

by a separation of variable technique, namely, let $T = f(x)h(z)$ where:

$$z = \frac{r}{R} \alpha Pr^{\frac{1}{2}}$$

$$\alpha = i^{\frac{3}{2}} R\left(\frac{\rho_o \omega}{\mu}\right)^{\frac{1}{2}}$$

$$Pr = \text{Prandtl number} = \frac{\mu g C_p}{\lambda} .$$

Equation (A.06) becomes a form of Bessel's equation, namely:

$$\frac{d^2h(z)}{dz^2} + \frac{1}{z}\frac{dh(z)}{dz} + h(z) = \frac{p}{\rho_o g C_p} \cdot \frac{1}{f(x)} \qquad (A.08)$$

which has a solution of the form:

$$h(z) = C_1 J_o(z) + C_2 Y_o(z) + \frac{p}{\rho_o g C_p} \cdot \frac{1}{f(x)} . \qquad (A.09)$$

From equation (A.07b) it follows that $C_2 = 0$. Since at $r = R$, $T = 0$, the function $f(x)$ may be determined:

$$f(x) = -\frac{1}{C_1 J_o(\alpha Pr^{\frac{1}{2}})} \cdot \frac{p(x)}{\rho_o g C_p} . \qquad (A.10)$$

Combining equations (A.09) and (A.10) yields an expression for the variation of the temperature perturbation amplitude as:

$$T = f(x)h(z) = \left[1 - \frac{J_o(\frac{r}{R} \alpha Pr^{\frac{1}{2}})}{J_o(\alpha Pr^{\frac{1}{2}})}\right] \frac{p(x)}{\rho_o g C_p} . \qquad (A.11)$$

It should be noted that the Bessel functions of equation (A.11) have complex arguments due to the presence of $i^{\frac{3}{2}} = e^{\frac{3\pi i}{4}}$ in the α constant; hence we introduce the Kelvin functions:

$$\left.\begin{aligned} &J_o(y\, i^{\frac{3}{2}}) = \text{ber } y + i \text{ bei } y \\ &\text{or alternatively in terms of amplitude and phase:} \\ &J_o(y\, i^{\frac{3}{2}}) = M_o(y)\,[\cos\theta_o(y) + i\ \sin\theta_o(y)] . \end{aligned}\right\} \qquad (A.12)$$

The first of the linearized Navier-Stokes equations, equation (A.02), can be similarly solved for the amplitude of the axial velocity

perturbation, resulting in:

$$u = \left[\frac{J_o(\frac{r}{R}\alpha)}{J_o(\alpha)} - 1\right] \frac{1}{i\omega\rho_o} \frac{dp}{dx} . \tag{A.13}$$

Substitution of the temperature variation, equation (A.11), into the equation of state yields:

$$\rho = \frac{\gamma}{a^2_o} p \left\{1 - \frac{\gamma-1}{\gamma}\left[1 - \frac{J_o(\frac{r}{R}\alpha Pr^{1/2})}{J_o(\alpha Pr^{1/2})}\right]\right\}. \tag{A.14}$$

Finally, the equation of continuity, equation (A.04), can be considered using the results for the axial velocity and density perturbations, equations (A.13) and (A.14), respectively; this becomes:

$$\frac{1}{r}\frac{\partial(rv)}{\partial r} = \frac{1}{i\omega\rho_o}\left\{\frac{\omega^2}{a^2_o}\gamma p\left[1 - \frac{\gamma-1}{\gamma}\left(1 - \frac{J_o(\frac{r}{R}\alpha Pr^{1/2})}{J_o(\alpha Pr^{1/2})}\right)\right]\right.$$

$$\left. - \frac{d^2p}{dx^2}\left[\frac{J_o(\frac{r}{R}\alpha)}{J_o(\alpha)} - 1\right]\right\}. \tag{A.15}$$

Equation (A.15) may be integrated with respect to r in order to find $(r\cdot v)$ with an arbitrary functional F(x) upon recognition that:

$$\frac{d}{dy}[yJ_1(y)] = yJ_o(y) .$$

Hence:

$$(r\cdot v) = \frac{1}{i\omega\rho_o}\left\{\frac{\omega^2}{a^2_o}\gamma p\left[\frac{1}{2}r^2 - \frac{\gamma-1}{\gamma}\left(\frac{1}{2}r^2 - \frac{rR}{\alpha Pr^{1/2}}\frac{J_1(\frac{r}{R}\alpha Pr^{1/2})}{J_o(\alpha Pr^{1/2})}\right)\right]\right.$$

$$\left. - \frac{d^2P}{dx^2}\left[\frac{rR}{\alpha}\frac{J_1(\frac{r}{R}\alpha)}{J_o(\alpha)} - \frac{1}{2}r^2\right] + F(x)\right\}. \tag{A.16}$$

Applying the boundary condition, y(x,R) = 0, one obtains:

$$F(x) = -\frac{\omega^2}{a^2_o}\gamma\frac{R^2}{2} p\left[1 + \frac{\gamma-1}{\gamma}\frac{J_2(\alpha Pr^{1/2})}{J_o(\alpha Pr^{1/2})}\right] - \frac{R^2}{2}\frac{J_2(\alpha)}{J_o(\alpha)}\frac{d^2p}{dx^2} \tag{A.17}$$

where the Bessel function of the first kind and second order is obtained from the recurrence relation:

$$J_2(y) = \frac{2\,J_1(y)}{y} - J_0(y) \ .$$

Consideration of equation (A.16) in the limit when the radial coordinate, r, tends to zero requires that the constant F(x) equal zero, yielding the governing ordinary second order differential equation for the pressure perturbation:

$$\frac{\omega^2}{a^2_0}\,\gamma p\left[1 + \frac{\gamma-1}{\gamma}\,\frac{J_2(\alpha Pr^{1/2})}{J_0(\alpha Pr^{1/2})}\right] - \frac{J_2(\alpha)}{J_0(\alpha)}\,\frac{d^2p}{dx^2} = 0 \ . \qquad \text{(A.18)}$$

The homogeneous equation provides a solution for the pressure perturbation:

$$p = A\,\exp(\phi x) + B\,\exp(-\phi x) \qquad \text{(A.19)}$$

where:

$$\phi = \frac{\omega}{a_0}\,\frac{J_0^{1/2}(\alpha)}{J_2^{1/2}(\alpha)}\,\gamma^{1/2}\left[1 + \frac{\gamma-1}{\gamma}\,\frac{J_2(\alpha Pr^{1/2})}{J_0(\alpha Pr^{1/2})}\right]^{1/2} \ .$$

The constants A and B may be determined after the boundary conditions at both ends of the tube have been prescribed, in addition to assumptions dealing with the instrument volume, namely:

a. Pressure and density in the instrument volumes are only time dependent, and

b. The pressure expansion in the instrument volume is a polytropic process, described by:

$$\frac{\bar{P}_v}{(\bar{\rho}_v)^k} = \text{constant} \ . \qquad \text{(A.20)}$$

Consider the system as sketched below in a sectional view:

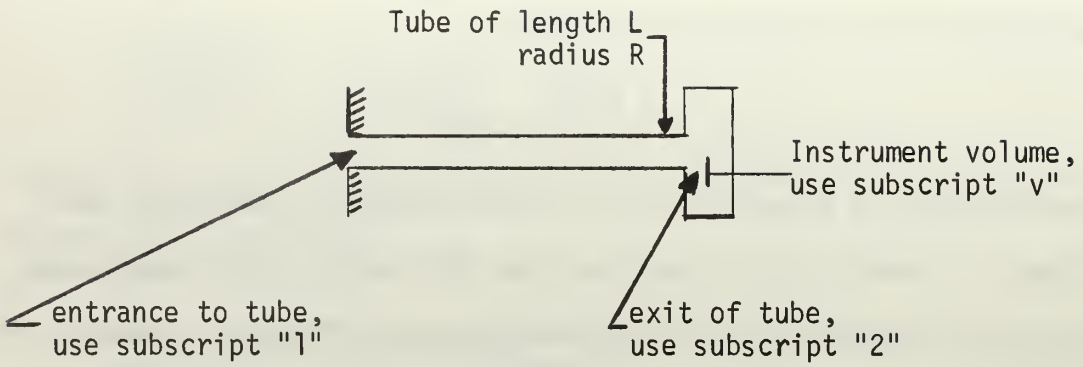

If the length of the tube is L, then the pressure at the inlet, station 1, and at the exit, station 2, is given by equation (A.19) as:

$$P_1 = A + B$$

$$P_2 = A \exp(\phi L) + B \exp(-\phi L) \; . \qquad \text{(A.21a)}$$

The constants A and B can be expressed in terms of P_1 and P_2 as:

$$A = \frac{-1}{2 \sinh(\phi L)} [P_1 \exp(-\phi L) - P_2]$$

$$B = \frac{1}{2 \sinh(\phi L)} [P_1 \exp(\phi L) - P_2 \;] \; . \qquad \text{(A.21b)}$$

The instrument volume has an influence upon the pressure response and is brought into consideration by requiring that the mass flow at station 2, the tube exit, be in balance with the change in mass in the instrument cavity. The axial velocity amplitude at station 2 may be obtained by combining the pressure equation, equation (A.19), with the velocity solution, equation (A.13), to yield:

$$u_2 = \frac{-\phi}{i\omega\rho_o} \left[\frac{J_o(\frac{r}{R}\alpha)}{J_o(\alpha)} - 1 \right] \left[A \exp(\phi L) - B \exp(-\phi L) \right] . \qquad \text{(A.22)}$$

At x = L, the mass flow can be expressed in a harmonic form by a straightforward integration process:

$$m_2 e^{i\omega t} = e^{i\omega t} \int_0^R \rho_o u_2 (2\pi r) dr$$

$$m_2 e^{i\omega t} = \frac{\pi\phi}{i\omega} R^2 \frac{J_2(\alpha)}{J_o(\alpha)} [A \exp(\phi L) - B \exp(-\phi L)] e^{i\omega t} . \qquad (A.23)$$

On the assumption that the pressure perturbation in the instrument cavity is equal to that at the tube exit, $p_2 = p_v$, one obtains from a linear expansion of the polytropic relation of equation (A.20):

$$\frac{\bar{p}_v}{(\bar{\rho}_v)^k} = \text{constant} = \frac{p_o + p_v e^{i\omega t}}{(\rho_o + \rho_v e^{i\omega t})^k} = \frac{p_o}{(\rho_o)^k}$$

which simplifies to:

$$p_2 = a^2_o \frac{k}{\gamma} \rho_v . \qquad (A.24)$$

The mass in the instrument volume can be expressed in terms of the density under the assumption of constant volume. This assumption implies that the harmonic motion of the transducer diaphragm, which forms part of the cavity wall, is small. Hence:

$$m_v = v_v(\rho_o + \rho_v e^{i\omega t}) = v_v(\rho_o + \frac{\gamma}{a^2_o k} p_2 e^{i\omega t}) . \qquad (A.25)$$

By conservation of mass, it is clear that:

$$\frac{dm_v}{dt} = m_2 e^{i\omega t} . \qquad (A.26)$$

Combining equations (A.26), (A.23), and (A.21), one obtains:

$$\frac{i\omega\gamma}{a^2_o k} v_v p_2 = \frac{\pi\phi}{i\omega} R^2 \frac{J_2(\alpha)}{J_o(\alpha)} \frac{1}{\sinh(\phi L)} [-p_1 + p_2 \cosh(\phi L)]$$

or finally, the result for the dynamic response is obtained:

$$\frac{p_2}{p_1} = [\cosh(\phi L) + \frac{\omega^2}{a^2_o} \frac{\gamma}{k} \frac{v_v}{v_t} \frac{L}{\phi} \frac{J_o(\alpha)}{J_2(\alpha)} \sinh(\phi L)]. \qquad (A.27)$$

The formulation of equation (A.27) has been made by Bergh who has obtained good experimental confirmation. The frequency response is

significantly influenced by system geometry and mean pressure level, while the influence of the polytropic process index, k, was found by Bergh to be minor. In actual data reduction, one would take into account the value of mean static pressure in order to obtain a more precise definition of the dynamic response curve. This effect would be important in an experiment where the static pressure level might vary by more than about plus or minus 0.25 atmosphere.

It is not difficult, as shown by Bergh, to extend these results to a series hookup of tubes and volumes by a repetitive analysis where the frequency response for input and exit of each individual tube length is obtained separately. It would be interesting to determine if a series connection of several tubes and volumes could lead to a more flat frequency response curve. This remains as an area for future investigation.

APPENDIX B

PREDICTION OF UNSTEADY PRESSURES DUE TO HARMONICALLY OSCILLATING PLAIN FLAP

The analysis described here may be considered as classical in the area of incompressible inviscid unsteady aerodynamics and is attributable to Kussner and Schwarz [6]. An introduction to the method is described in the aeroelasticity test by Fung [7], and for that reason only the particular terms involved in developing a solution for the pressures in the presence of an oscillating plain flap will be treated here.

Consider a two-dimensional airfoil section of unit valued semi chord. A trigonometric coordinate transformation (sketched below) for chordal location may be used as is familiar in thin airfoil theory:

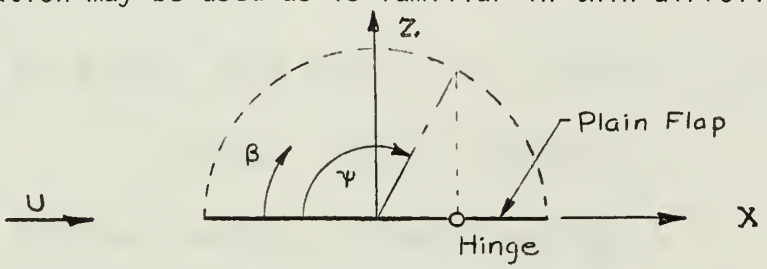

Let $x = -\cos\beta$ so that $x = -1$ at the leading edge, $\beta = 0$, and $x = +1$ at the trailing edge, $\beta = \pi$. The hinge line of the plain flap is located by the angle ψ.

The harmonic motion of the airfoil is defined by:

$$z = 0 \text{ for } 0 \leq \beta \leq \psi$$

and

$$z = \delta(\cos\psi - \cos\beta)e^{i\omega t} \text{ for } \psi \leq \beta \leq \pi \ .$$

The downwash on the mean line can be described by:

$$v(x,t) = U\frac{\partial z}{\partial x} + \frac{\partial z}{\partial t}$$

or in trigonometric notation for the case of the oscillating plain flap:

$$v(\beta,t) = U\delta e^{i\omega t}[ik(\cos\psi - \cos\beta) + 1] \qquad (B.01)$$

where again $\psi \leq \beta \leq \pi$ and the non-dimensional frequency term is:

$$k = \frac{\omega}{U} \qquad (\frac{c}{2} = 1) \ .$$

With this notation, a solution for the unsteady pressure developed at a chordal location corresponding to the angle β can be developed after considerable analysis. The results of Kussner and Schwarz can be summarized for the dimensionless pressure differential as:

$$\Delta Cp(\beta,t) = \frac{4}{\pi}\,\delta e^{i\omega t}[Re(k,\beta,\psi) + iIm(k,\beta,\psi)] \qquad (B.02)$$

where

$Re\ (k,\beta,\psi)$ = Real part of expression

$Im\ (k,\beta,\psi)$ = Imaginary part of expression

and

$$\begin{aligned} Re\ (k,\beta,\psi) = {} & [F(k)\ \Phi_1(\psi) - \frac{k}{2}\,G(k)\ \Phi_2(\psi) - \sin\psi]\cot\frac{\beta}{2} \\ & + L(\beta,\psi)[1 + 2(\cos\psi - \cos\beta)] \\ & - \frac{k^2}{2}\{[(\pi-\psi)2\cos\psi + \sin\psi]\sin\beta - (\pi-\psi)\sin\beta\cos\beta \\ & + L(\beta,\psi)(\cos\psi - \cos\beta)^2\} \end{aligned} \qquad (B.03a)$$

$$\begin{aligned} Im\ (k,\beta,\psi) = {} & [G(k)\Phi_1(\psi) + \frac{k}{2}\,F(k)\Phi_2(\psi) - \frac{k}{2}\Phi_3(\psi)]\cot\frac{\beta}{2} \\ & + 2k(\pi-\psi)\sin\beta. \end{aligned} \qquad (B.03b)$$

In equations (B.02a) and (B.02b), we further identify that:

$F(k) + G(k) = C(k)$ = Theodorsen coefficient which is tabulated in Reference [7] and:

$$L(\beta,\psi) = \frac{1}{2} \ln \frac{1-\cos(\beta+\psi)}{1-\cos(\beta-\psi)}$$

$$\Phi_1(\psi) = (\pi-\psi) + \sin\psi$$

$$\Phi_2(\psi) = (\pi-\psi)(1+2\cos\psi) + \sin(2+\cos\psi)$$

$$\Phi_3(\psi) = (\pi-\psi) + \sin\psi\cos\psi$$

A set of calculations were made to correspond to the wind-tunnel experiment, namely, the pressures at the 75 per cent chord station in the presence of an oscillating 20 per cent chord radius nosed plain flap. Results of the calculations relative to amplitude change and phase angle for the pressure differential are shown on Figure 16 where the values are normalized relative to the k = 0 (stationary flap on a fixed airfoil) situation.

APPENDIX C

X-Z COORDINATES OF THE NACA 64_1-012 MODIFIED AIRFOIL USED IN THE WIND TUNNEL TESTS OF THE UNSTEADY PRESSURE MEASURING SYSTEM

STATION	X - INCHES	Z - INCHES
0	0.00	0
1	.06	0.11736
2	.09	.14148
3	.15	.17880
4	.30	.24420
5	.60	.3372
6	.90	.40716
7	1.20	.46452
8	1.80	.55440
9	2.40	.62076
10	3.00	.66912
11	3.60	.70128
12	4.20	.71736
13	4.80	.71772
14	5.40	.69576
15	6.00	.65760
16	6.60	.60672
17	7.20	.54576
18	7.80	.48129
19	8.40	.41682
20	9.00	.35235
21	9.60	.28788
22	10.20	.22341
23	10.80	.15894
24	11.40	.09447
25	12.00	0.03000

INITIAL DISTRIBUTION LIST

		No. Copies
1.	Defense Documentation Center Cameron Station Alexandria, Virginia 22314	20
2.	Library Naval Postgraduate School Monterey, California 93940	2
3.	Professor Louis V. Schmidt Department of Aeronautics Naval Postgraduate School Monterey, California 93940	5
4.	Chairman, Department of Aeronautics Naval Postgraduate School Monterey, California 93940	1
5.	Professor Allen E. Fuhs Department of Aeronautics Naval Postgraduate School Monterey, California 93940	1
6.	Professor James A. Miller Department of Aeronautics Naval Postgraduate School Monterey, California 93940	1
7.	Superintendent U. S. Naval Academy Annapolis, Maryland 21402	1
8.	Head of Engineering Department U. S. Naval Academy Annapolis, Maryland 21402	1
9.	Office of Naval Research Air Programs Office Navy Department Washington, D. C. 20360	1
10.	Commander Naval Ordnance Systems Command Navy Department Washington, D. C. 20360	1
11.	Commander Naval Air Systems Command Navy Department Washington, D. C. 20390	1

		No. Copies
12.	Dr. E. S. Lamar (Code 03C) Chief Scientist, Research and Technology Naval Air Systems Command Navy Department Washington, D. C. 20390	1
13.	Mr. G. L. Desmond (Code 320) Aerodynamics and Structures Administration Research and Technology Naval Air Systems Command Navy Department Washington, D. C. 20390	1
14.	Dr. F. I. Tanczos Technical Director, Research and Technology Naval Air Systems Command Navy Department Washington, D. C. 20390	1
15.	Mr. Paul Fisher Special Projects Office Navy Department Washington, D. C. 20360	1
16.	Lieutenant Ronald B. Johnson 433 Casa Verde, Apt. 128 Monterey, California 93940	3

DOCUMENT CONTROL DATA - R & D

Security classification of title, body of abstract and indexing annotation must be entered when the overall report is classified)

1. ORIGINATING ACTIVITY *(Corporate author)*

Naval Postgraduate School
Monterey, California 93940

2a. REPORT SECURITY CLASSIFICATION

UNCLASSIFIED

2b. GROUP

3. REPORT TITLE

A Technique for Measuring Unsteady Pressure

4. DESCRIPTIVE NOTES *(Type of report and inclusive dates)*

Engineer's Thesis

5. AUTHOR(S) *(First name, middle initial, last name)*

Ronald B. Johnson, Lieutenant, USN

6. REPORT DATE	7a. TOTAL NO. OF PAGES	7b. NO. OF REFS
September, 1968	61	7

8a. CONTRACT OR GRANT NO	9a. ORIGINATOR'S REPORT NUMBER(S)
b. PROJECT NO.	
c.	9b. OTHER REPORT NO(S) *(Any other numbers that may be assigned this report)*
d.	

10. DISTRIBUTION STATEMENT

[redacted]

11. SUPPLEMENTARY NOTES	12. SPONSORING MILITARY ACTIVITY
	Naval Postgraduate School Monterey, California 93940

13. ABSTRACT

A system for measuring unsteady pressures in flow fields employing a remote transducer and thin plastic pressure transmitting lines has been designed and built.

The static and dynamic characteristics of the system were determined experimentally, and the results were found to agree well with a theoretical model.

The measuring system was subsequently integrated into a two-dimensional wind tunnel model consisting of a symmetrical airfoil with a plain oscillating flap. The flap was harmonically oscillated, and the measuring system was used to determine both the steady and unsteady pressures at a point near the flap hinge line. The static and dynamic results were then compared to those obtained using thin airfoil theory and found to agree well when corrected for thickness effects.

14 KEY WORDS	LINK A		LINK B		LINK C	
	ROLE	WT	ROLE	WT	ROLE	WT
Unsteady pressure						
Pressure measurements						
Oscillating plain flap						
Pressure transducers